Nondemolition quasiprobabilities of work and heat in the presence of a non-Markovian environment

Haiping Li, Jian Zou[*] and Bin Shao

Key Laboratory of Advanced Optoelectronic Quantum Architecture and Measurement, Ministry of Education,
School of Physics, Beijing Institute of Technology, Beijing 100081, China

We consider a collision model representation of nonequilibrium dynamics for an externally driven open quantum system. Specifically we investigate the nondemolition quasiprobability distributions (QPDFs) of work and heat in both Markovian and non-Markovian regimes. In this model, work and heat correspond to different evolution processes, and their contributions can be distinguished. For the system state with initial coherence, in both Markovian and non-Markovian regimes, negative quasiprobabilities at half of the energy gap of the system for work and the variation of internal energy appear, which is considered to be a witness of the quantumness of the system. We also find that when the external driving speed slows down, the quantumness of the system is weakened, and when the driving speed is slow enough, the negative quasiprobability will disappear and the results of the QPDF coincide with those of the two-measurement protocol. Most importantly, we find that non-Markovianity can enhance the quantumness of the system.

DOI: 10.1103/PhysRevA.109.032228

I. INTRODUCTION

In the past decades, there has been growing interest regarding the applicability of thermodynamics to microscopic systems, particularly at the nanoscale [1,2]. Quantum effects, such as quantum coherence [3–8] and quantum correlations [9–12], play a significant role in microscopic systems. Efforts have been made to use the characteristics of quantum effects to achieve more efficient energy extraction in quantum systems than in classical systems [13]. In addition, fluctuations play an important role in thermodynamics of small systems. Thus, it is necessary to study the probability distributions of work and heat, as their average value cannot sufficiently describe the dynamics.

Numerous proposals have been put forward to characterize the probability distributions of work. Among these, the most widely used measurement proposal is based on the two-point measurement (TPM) protocol [14–19]. However, the initial coherence of the system is destroyed by the first projective measurement, thus the TPM is not applicable to give a thermodynamically consistent description of the work distribution for an initial state with quantum coherence [20]. Additionally, other methods beyond the TPM have been proposed, such as the work operator [21], Gaussian measurement [22], consistent histories [23], weak values [24], full counting statistics [25], Kirkwood-Dirac quasiprobability [26], Margenau-Hill quasiprobability [27], and a general notion of quasiprobability [28] in analogy to the well-known Gleason's theorem [29]. On the other hand, quantum heat is usually associated with nonunitary parts of the dynamics [30,31], representing the classical energy exchange with the environment. The proposals to obtain the quantum heat

statistics have been given in some literatures, including single discrete quantum jumps [32,33], single continuous quantum trajectories [34,35], path integrals formulation [36,37], full counting statistics [25,38], and quantum Bayesian network [39]. Besides, other methods—for example end-point measurement and one-time measurement based on guessed work and heat—have been proposed to characterize the energy-change statistics [40,41].

Recently, a detection scheme to obtain the quasiprobability density distribution function (QPDF) of work and heat was proposed by Solinas and Gasparinetti [42–44]. Coupling the system and the detector allows the information about the physical observable of the system to be stored in the phase of the quantum detector, and the quasi-characteristic generating function (QCGF) and QPDF can be obtained by measuring the phase of the detector. Unlike previous methods, the statistics of work and heat can be measured by accessing the degrees of freedom of the system only. This offers a more accessible way to obtain the statistics of work and heat experimentally. Reference [13] implemented the scheme on an IBMQ device, and the QPDFs of work, heat, and the variation of internal energy in one cycle were obtained. Reference [45] presented a theoretical framework for QPDFs of work, heat, and the variation of internal energy in driven open systems, and discussed the QPDFs in the limit of closed evolution and fast dissipation.

In general, the evolution of an open system can be described by a quantum master equation with Markovian approximation [46], where there is only a monotonous information flow from the system to the environment. But when the memory effect of the environment cannot be ignored, i.e., there is an information backflow from the environment to the system, the dynamics is non-Markovian [47]. In addition, the memory effect is regarded as a resource in information theory [48–52], and has led to some interesting phenomena in the dynamics of open quantum systems [53–59]. So far, the study

*zoujian@bit.edu.cn

of the probability distribution of work and heat focused on the Markovian environments, but the effect of non-Markovianity on the probability distributions of work and heat is not clear and needs further study.

In this paper, we focus on a driven quantum system coupled to a thermal reservoir, which consists of a series of two-level ancillas. Non-Markovian evolution can be achieved by introducing the interactions between ancillas [60]. It is known that distinguishing work and heat in a general thermodynamics process when both drive and dissipation exist is a challenge. In this model, the contributions of work and heat can be well distinguished because work and heat are associated with different dynamical evolutions. We find that for the system state with initial coherence, whether for a Markovian environment or a non-Markovian environment, negative QPDFs at half of the energy gap of the system for work and the variation of internal energy appear, which is considered to be a witness of the quantumness of the system. When there is no interaction between ancillas, i.e., the system is Markovian, we find that the change of the environmental temperature has little effect on the quantumness of the system. Additionally, we note that as the external driving speed slows down, the quantumness of the system is weakened. When the driving speed is slow enough, the negative quasiprobability vanishes, and the outcomes of the QPDF return to those of the TPM. Furthermore, the coupling between the system and the environment destroys the initial coherence of the system, resulting in the weakened quantumness of the system. When considering the case where the coupling between ancillas is not zero, i.e., the memory effect comes into play, we find that the stronger the non-Markovianity, the stronger the quantumness of the dynamics.

II. PRELIMINARIES

In this section, we introduce the model used in this paper and the TPM for calculating work, heat, and the variation of internal energy of the quantum system. In Sec. II A we introduce the model, and in Sec. II B we derive the probability distributions of work, heat, and the variation of internal energy of the system by the TPM for our model.

A. Model

Let us consider an open two-level system denoted by S subjected to a time-dependent drive, and the total time-dependent Hamiltonian of the system at time t is

$$H_S(t) = \frac{1}{2}\omega\sigma_z^S + \frac{1}{2}g\big(\sigma_x^S\cos\omega t + \sigma_y^S\sin\omega t\big). \quad (1)$$

In this paper, we set $\hbar = 1$. In Eq. (1) the first term represents the free Hamiltonian of the system and the remaining of Eq. (1) represents the external driving acting on the system. In the operators σ_i^S, $i = x, y, z$ are the usual Pauli operators of the system. ω is the energy gap of the qubit during free evolution and also the driving frequency of the two-level system, and g is the driving intensity quantifying the coupling to the external field. The instantaneous eigenvalues and eigenvectors of the system are labeled as $\varepsilon_i(t)$ and $|i(t)\rangle$, respectively, satisfying

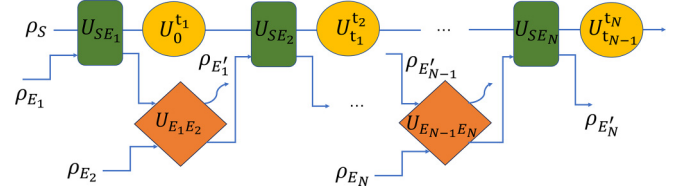$$H_S(t)|i(t)\rangle = \varepsilon_i(t)|i(t)\rangle, \quad (2)$$

FIG. 1. N steps of the evolution process for an open quantum system under an external drive. The system evolves under an external drive, interrupted by the S-E interaction and AA interaction. In the first step, the system interacts with the E_1, next E_1 interacts with E_2, then the system evolves from 0 to t_1 under the unitary evolution $U_0^{t_1}$. In the next step, the system interacts with E_2, E_2 interacts with E_3, the system evolves from t_1 to t_2, and so on.

where $i = g, e$, and $|g(t)\rangle$, $|e(t)\rangle$ are the instantaneous ground state and excited state of the system at time t. And, the Hamiltonian varies with time, guaranteeing that the external field does work on the system. It should be noted that for the Hamiltonian in Eq. (1), although the eigenstates of the system may change with time, the eigenvalues of the system energy remain unchanged, i.e.,

$$\varepsilon_e(t) = -\varepsilon_g(t) = \frac{\sqrt{\omega^2 + g^2}}{2} \equiv \frac{\varepsilon}{2}. \quad (3)$$

And, the corresponding unitary operator U_S generated by the Hamiltonian $H_S(t)$ is [61,62]

$$\begin{aligned}
U_S(t) &= \mathcal{T}\exp\left(-i\int_0^t dt H_S(t)\right) \\
&= \begin{pmatrix} \cos\frac{gt}{2}e^{-i\frac{\omega t}{2}} & -i\sin\frac{gt}{2}e^{-i\frac{\omega t}{2}} \\ -i\sin\frac{gt}{2}e^{i\frac{\omega t}{2}} & \cos\frac{gt}{2}e^{i\frac{\omega t}{2}} \end{pmatrix},
\end{aligned} \quad (4)$$

where $\mathcal{T}$ is the time-ordering operator.

To describe the influence of the environment, we use the collision model [60,63], which is efficient for describing dissipation dynamics. The collision model assumes that the environment is composed of a large number of initially uncorrelated ancillas, and both Markovian and non-Markovian dynamics can be simulated by adjusting the relevant parameters [60]. In Markovian dynamics, there is only an information flow from the system to the environment, but if there is an information flow back from the environment to the system, the system may get former information about itself, and the dynamics is non-Markovian. In this paper, the collision model involves a time-dependent drive that acts on the system, and the drive is interrupted by the system-environment (S-E) interactions and the ancilla-ancilla (AA) interactions, as shown in Fig. 1. In Fig. 1, in the first step, at time $t_0 = 0$ the system interacts with E_1, E_1 interacts with E_2, and the system evolves to t_1 under the unitary evolution $U_S(t)$; in the next step, the system interacts with E_2, E_2 interacts with E_3, and then the system evolves from t_1 to t_2, and so forth. The memory effect is introduced by the AA interactions. In the absence of interactions between ancillas, there is no backflow of information from the environment to the system, and the dynamics is Markovian. However, when there are interactions between ancillas, the system will interact with the nth ancilla carrying the information obtained from the previous $n - 1$

collisions, and the information from the previous process may participate in the dynamics of the system, thus this process may be non-Markovian.

We assume that the evolution occurs for $0 \leqslant t \leqslant t_N$, and discretize it in N steps, labeled in discrete time instant $t = t_0, t_1, t_2, \ldots, t_N$, where $t_n = n\Delta t = n t_N/N$. Here, we introduce the concept of driving speed $v = \|\Delta H_S\|/N$, where $\|\Delta H_S\|$ represents the norm of the variation of the system Hamiltonian $H_S(t)$ [64]. To simplify the expression, the eigenvalues $\varepsilon_i(t_n)$ and eigenvectors $|i(t_n)\rangle$ of the system at time t_n are substituted by ε_{i_n} and $|i_n\rangle$, respectively. In addition, we assume that each ancilla E_n is a two-level qubit with the same free Hamiltonian $H_{E_n} = \frac{\varepsilon}{2}\sigma_z$, where ε is the energy gap of an ancilla, which is equal to the energy gap of the Hamiltonian $H_S(t)$ in Eq. (1). We also assume that each ancilla is in the same initial state ρ_{E_n}. We label the eigenvalues and eigenvectors of the ancillas as $H_{E_n}|f_n\rangle = \varepsilon_{f_n}|f_n\rangle$, where $f = g, e$. As an example we consider the interaction between the system and the nth ancilla, and assume that the interaction Hamiltonian between the system and E_n is

$$H_{SE_n} = \Lambda\big(\sigma_S^+(t_{n-1})\sigma_{E_n}^- + \sigma_S^-(t_{n-1})\sigma_{E_n}^+\big), \quad (5)$$

where Λ represents the S-E coupling strength; $\sigma_S^+(t_{n-1})$ and $\sigma_S^-(t_{n-1})$ denote the raising and lowering operators of the system at t_{n-1}, respectively; and $\sigma_{E_n}^+$ and $\sigma_{E_n}^-$ are the raising and lowering operators of the nth ancilla, respectively. It is worth noting that at time t_0, the system interacts with the first ancilla, and at time t_{n-1}, the system interacts with the nth ancilla. The overall evolution operator can be written as

$$U_{SE_n} = e^{-i\Lambda\delta t_1\big(\sigma_S^+(t_{n-1})\sigma_{E_n}^- + \sigma_S^-(t_{n-1})\sigma_{E_n}^+\big)}, \quad (6)$$

where δt_1 is the time interval of the interaction between the system and the ancilla. In fact, when $H_S(t_{n-1}) + H_{E_n}$ do not commute with H_{SE_n}, not only will there be an exchange of heat between the two qubits, but the work will also be generated during the interaction. Our choice of $H_S(t)$ in Eq. (1) ensures

that $[H_S(t_{n-1}) + H_{E_n}, H_{SE_n}] = 0$ at any time, therefore there is only heat exchange between the system and the environment. Thus, when the system interacts with the ancilla E_n, the overall system-environment evolution U_{SE_n} satisfies the strong energy-preservation condition [39], there are no other energy transformations involved, and all the change in the energy of the system can be unambiguously identified as heat flowing to the environment.

The interaction Hamiltonian between the $(n-1)$th ancilla and the nth ancilla is assumed as

$$H_{E_{n-1}E_n} = \Gamma\big(\sigma_{E_{n-1}}^+\sigma_{E_n}^- + \sigma_{E_{n-1}}^-\sigma_{E_n}^+\big), \quad (7)$$

and the evolution operator is

$$U_{E_{n-1}E_n} = e^{-i\Gamma\delta t_2\big(\sigma_{E_{n-1}}^+\sigma_{E_n}^- + \sigma_{E_{n-1}}^-\sigma_{E_n}^+\big)}, \quad (8)$$

where Γ represents the coupling strength between ancillas and δt_2 is the time interval of the interaction between ancillas. It can be found that for the evolution operator of the AA interaction introduced in Eq. (8), the dynamics vary periodically with the coupling strength between ancillas. In this paper, we focus on the dynamics in the interval $0 \leqslant \Gamma \leqslant \frac{\pi}{2}$, where the coupling between ancillas is enhanced as Γ increases. If the AA coupling strength $\Gamma = 0$, the dynamics is Markovian, and when the AA coupling strength $\Gamma \neq 0$, the dynamics might be non-Markovian. Additionally, we assume that the S-E coupling and AA coupling occur on much smaller timescales with respect to the driving timescale, i.e., δt_1, $\delta t_2 \ll \Delta t$. Under this condition, in every time interval $\delta t_1 + \delta t_2$, the Hamiltonian of the system can be considered unchanged. Hence, when the interactions between the system and the ancillas and the interactions between ancillas occur, the free evolution of the system and the drive action on the system can be ignored. Thus, the total evolution of the system from t_{n-1} to t_n can be written in terms of the unitary evolution experienced by the system and environment,

$$\rho_1^{SE} = U_1\big(\rho_{S_0}\bigotimes\rho_{E_1}\bigotimes\rho_{E_2}\big)U_1^\dagger = U_0^{t_1}U_{E_1E_2}U_{SE_1}\big(\rho_{S_0}\bigotimes\rho_{E_1}\bigotimes\rho_{E_2}\big)U_{SE_1}^\dagger U_{E_1E_2}^\dagger\big(U_0^{t_1}\big)^\dagger,$$

$$\rho_n^{SE} = U_n\big(\mathrm{Tr}_{E_{n-1}}\big[\rho_{n-1}^{SE}\big]\bigotimes\rho_{E_{n+1}}\big)U_n^\dagger = U_{t_{n-1}}^{t_n}U_{E_nE_{n+1}}U_{SE_n}\big(\mathrm{Tr}_{E_{n-1}}\big[\rho_{n-1}^{SE}\big]\bigotimes\rho_{E_{n+1}}\big)U_{SE_n}^\dagger U_{E_nE_{n+1}}^\dagger\big(U_{t_{n-1}}^{t_n}\big)^\dagger (n > 1), \quad (9)$$

where $\mathrm{Tr}_{E_{n-1}}[\bullet]$ represents tracing out the $(n-1)$th ancilla before the system interacts with the nth ancilla. It is important to note that $\mathrm{Tr}_{E_{n-1}}[\rho_{n-1}^{SE}]$ is the overall state of the system and the nth ancilla, $U_0^{t_1} = U_S(t_1)$ and $U_{t_{n-1}}^{t_n} = U_S(t_n)U_S^\dagger(t_{n-1})$. It should be noted that only when the ancilla has completely run out of its usefulness—in other words, it will not participate in the subsequent evolution of the dynamics—can it be traced out. The reduced state of the system after interacting with a set of n ancillas is obtained by taking the partial trace over the degrees of freedom of the ancillas,

$$\rho_{S_n} = \mathrm{Tr}_{E_nE_{n+1}}\big[\rho_n^{SE}\big]. \quad (10)$$

And, the reduced state of the nth ancilla after interaction is

$$\rho_{E_n'} = \mathrm{Tr}_{SE_{n+1}}\big[\rho_n^{SE}\big], \quad (11)$$

where $\mathrm{Tr}_{E_nE_{n+1}}[\bullet]$ represents tracing out the nth ancilla and the $(n+1)$th ancilla, and $\mathrm{Tr}_{SE_{n+1}}[\bullet]$ represents tracing out the system and the $(n+1)$th ancilla.

B. Probability distributions of work, heat, and the variation of internal energy for TPM

In the following, unless specified otherwise, the system is initially described by the density matrix $\rho_{S_0} = \sum_{i_0 j_0}\rho_{i_0 j_0}|i_0\rangle\langle j_0|$, where $|i_0\rangle, |j_0\rangle = g(0), e(0)$ represent the Hamiltonian eigenstates of the system at time $t = 0$. And, the nth ancilla is prepared at the thermal state $\rho_{E_n} = \sum_{f_n}\rho_{f_n f_n}|f_n\rangle\langle f_n|$, where $|f_n\rangle$ represents the Hamiltonian eigenstate of the ancilla and $f_n = g_n, e_n$. The TPM is widely used to obtain the probability distribution of work, heat, and

the variation of internal energy. Since the internal energy is a function of system state, its variation is process independent. Therefore, we only need to know the energy of the initial and final states of the system to obtain the change of internal energy. However, the heat and work are not state functions and depend on the path swept by the system during the evolution. In this model, work and heat are associated with different dynamic processes, respectively. When the system and the environment interact, no work is done on the system and only the dissipative heat is involved. Therefore, all the variation in the energy of the system in this time interval can be interpreted as heat. And, when the system evolves under the drive of the time-dependent Hamilton $H_S(t)$, there is no energy exchange between the system and the environment, thus the energy change of the system in this process is defined as work. If the system is measured directly, the coherence of the system will inevitably be destroyed. We can obtain information of the system by measuring the state of the ancilla after it has outlived its usefulness and will not participate in the dynamic evolution. The nth ancilla is measured in its Hamiltonian eigenbasis for the first measurement before entering the dynamics evolution, whose result is labeled as $|f_n\rangle$. The nth ancilla is measured finally only after the ancilla has outlived its usefulness, whose result is labeled as $|f_n'\rangle$. And, the system is measured in the eigenstates of the time-dependent Hamiltonian $H_S(t_0)$ and $H_S(t_N)$ before and after the entire evolution of the system, whose results are labeled as $|i_0\rangle$ and $|i_N\rangle$. Based on the above measurement scheme, the corresponding quantum trajectory can be represented as

$$\gamma = \{i_0, f_1, f_1', f_2, f_2', \ldots, f_N, f_N', i_N\}. \tag{12}$$

After the first measurement $M_{f_n} = |f_n\rangle\langle f_n|$ on the nth ancilla, the probability of the outcome f_n is $P_{f_n} = \mathrm{Tr}[M_{f_n}\rho_{E_n}M_{f_n}^\dagger]$, and the ancilla state after the first measurement becomes $\rho_{f_n} = |f_n\rangle\langle f_n|$. Similarly, the probability of obtaining i_0 by measuring the initial state of the system before the evolution of the system is $P_{i_0} = \mathrm{Tr}(M_{i_0}\rho_{S_0}M_{i_0}^\dagger)$, where $M_{i_0} = |i_0\rangle\langle i_0|$ is measurement operator acting on the system, and the corresponding system state changes to $\rho_{i_0} = |i_0\rangle\langle i_0|$. Then, the joint distribution $P(\gamma)$ is given by

$$P(\gamma) = P_{i_0}P_{f_1}...P_{f_N}\mathrm{tr}_{SE_1...E_N}\left[M_{i_N}M_{f_N'}...M_{f_1'}U_N...U_1\left(\rho_{i_0} \otimes \rho_{f_1} \otimes ... \otimes \rho_{f_N}\right)U_1^\dagger...U_N^\dagger M_{f_1'}^\dagger...M_{f_N'}^\dagger M_{i_N}^\dagger\right]. \tag{13}$$

In this way, the variation of internal energy ΔU as the difference between the energy of the initial state and the final measured state of the quantum trajectory γ can be obtained,

$$\Delta U[\gamma] = \varepsilon_{i_N} - \varepsilon_{i_0}, \tag{14}$$

where ε_{i_n} represents the energy eigenvalue of the system at t_n. In the nth step, the heat can be defined for the trajectory in Eq. (12) as the sum of the energy change between final and initial states of the nth ancilla. After the interaction between the system and Nth ancilla, the total heat flow from the system to the environment is

$$Q[\gamma] = \sum_{n=1}^{N} \varepsilon_{f_n'} - \varepsilon_{f_n}. \tag{15}$$

It should be noted that an absorption (emission) by the environment corresponds to an emission (absorption) process of the system, i.e., decreasing (increasing) of the system energy. As the measurements are performed only on those ancillas that no longer participate in the dynamics of the system, there is never a direct back action on the system. And, it is irrelevant whether or not the measurement is taken before the next evolution step. In addition, according to the law of energy conservation, the work done on the system can be derived as $W[\gamma] = \Delta U[\gamma] + Q[\gamma]$.

III. QPDFS OF WORK, HEAT, AND THE VARIATION OF INTERNAL ENERGY

When the initial state of the system is in the energy eigenstate or a statistical mixture of energy eigenstates, the TPM is an effective method to determining the work, heat, and the variation of internal energy. But, it has its limitations when one tries to apply the TPM to a more general class of processes, i.e., the system is initially prepared in a superposition of different energy eigenstates. This limitation arises from the fact that the initial measurement destroys any initial coherence in the energy eigenbasis and consequently affects the results of work, heat, and the variation of internal energy. To preserve the information about the dynamics and the initial coherence of the system, a detection scheme QPDF was proposed by Solinas and Gasparinetti [42–44].

The QPDF protocol is to couple the system to a quantum detector, and the information about the system is stored in the phase of the detector. By measuring the phase shift of the detector, the QCGFs and QPDFs of work, heat, and the variation of internal energy can be obtained. When the system is initially in the eigenstate, the statistical information of the TPM is recovered. In this paper, the quantum detector is represented by an additional two-level qubit (denoted by D) with Hamiltonian $H_D = \sum_\lambda \lambda|\lambda\rangle\langle\lambda|$, where $\lambda = 0, 1$ and $|\lambda\rangle = \{|0\rangle, |1\rangle\}$ are the eigenvalues and eigenstates of the detector Hamiltonian. The detector is prepared in an arbitrary state $\rho_{D_0} = \sum_{\lambda,\lambda'} \rho_{\lambda\lambda'}|\lambda\rangle\langle\lambda'|$, where $\rho_{\lambda\lambda'}$ is the density matrix elements of the detector. And, the system-detector coupling Hamiltonian is chosen as

$$H_{SD} = f(\chi, t)H_S(t)\bigotimes H_D, \tag{16}$$

where the time-dependent coupling strength $f(\chi, t)$ determines the time when the system is coupled to the detector and the coupling strength χ between them. We assume that the system, environment, and detector are initially in a product state, which can be described by the factorized density
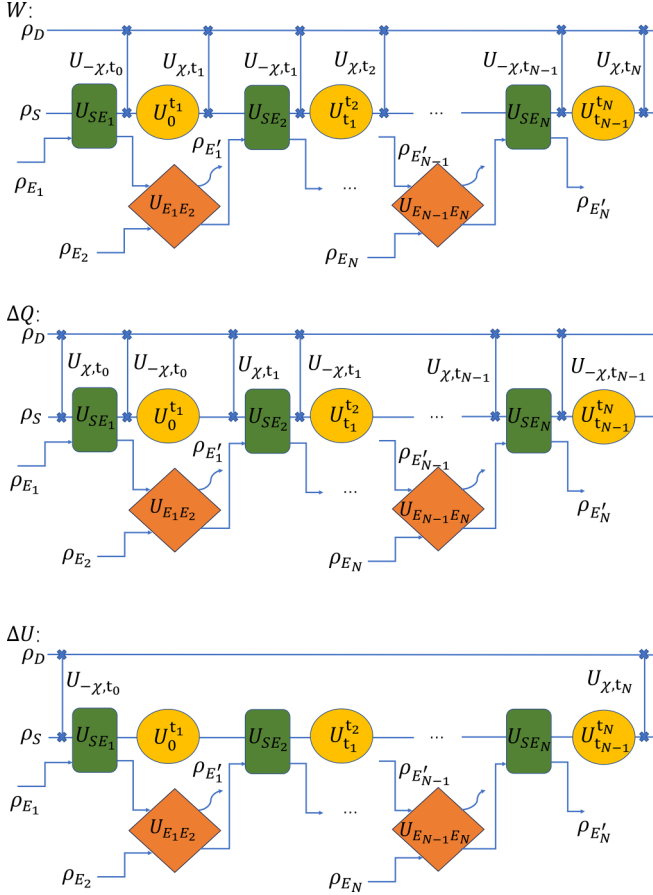
FIG. 2. Three schematic diagrams corresponding to the detection of the probability distributions of work W, heat ΔQ, and the variation of internal energy ΔU, respectively. For W: the system interacts with E_1, E_1 interacts with E_2, the system is coupled to the detector for the first time, the system evolves from 0 to t_1 under unitary evolution $U_0^{t_1}$, the system is coupled to the detector for the second time, and so forth. For ΔQ: the system is coupled to the detector for the first time, the system interacts with E_1, E_1 interacts with E_2, the system is coupled to the detector for the second time, the system evolves from 0 to t_1 under unitary evolution $U_0^{t_1}$, and so forth. For ΔU: the system and the detector are coupled at the beginning and end of the evolution, respectively.

operator,

$$
\begin{aligned}
\rho_0 &= \rho_{S_0} \bigotimes \rho_{E_1} \bigotimes \cdots \bigotimes \rho_{E_N} \bigotimes \rho_{D_0} \\
&= \sum \rho_{i_0 j_0} \rho_{f_1, h_1} \cdots \rho_{f_N, h_N} \rho_{\lambda \lambda'} \\
&\quad \times |i_0, f_1, \ldots, f_N, \lambda\rangle\langle j_0, h_1, \ldots, h_N, \lambda'|.
\end{aligned}
\tag{17}
$$

It is noted that during the whole process, neither the system nor the detector are projectively measured, and the specific choice of H_{SD} ensures that system-detector coupling does not lead to any transition between the instantaneous system eigenstates [44]. As mentioned above, the coupling between the system and the detector can change the relative phase of the detector, therefore the information about the physical observable is stored in the phase of the detector. Tracing out the system and environment degrees of freedom, the information about the observable can be obtained by extracting

the phase difference between the eigenstates $|\lambda\rangle$ and $|-\lambda\rangle$ of the detector. The QCGF for an arbitrary observable η is [43,44]

$$
\mathcal{G}_{\chi, \eta} = \frac{\langle\lambda|\rho_D(t_N)|-\lambda\rangle}{\langle\lambda|\rho_{D_0}|-\lambda\rangle},
\tag{18}
$$

and the final detector density operator $\rho_D(t_N)$ can be obtained as

$$
\rho_D(t_N) = \mathrm{Tr}_{SE}[\mathcal{U}_{\chi, \eta} \rho_0 \mathcal{U}_{\chi, \eta}^\dagger],
\tag{19}
$$

where $\mathcal{U}_{\chi, \eta}$ represents the total evolution operator of the system, environment, and detector, including the measurement of the detector, and the observable η could be W, Q, or ΔU. $\mathcal{U}_{\chi, \eta}$ is different for different observable η, and the specific form of $\mathcal{U}_{\chi, \eta}$ for $\eta = W, Q, \Delta U$ will be given in Secs. III A, III B, and III C, respectively. $\mathrm{Tr}_{SE}[\bullet]$ represents tracing out the degree of freedom of the system and all the ancillas. The QPDF can be obtained by taking the Fourier transform of the QCGF

$$
P(\eta) = \int d\chi \, \mathcal{G}_{\chi, \eta} e^{i\chi\eta}.
\tag{20}
$$

The QCGFs and the QPDFs of work, heat, and the variation of internal energy are given in the following.

A. QPDF of work

As mentioned above, work depends on the path swept by the system in the evolution process. To calculate the work done on the system from 0 to t_N, we must track the evolution in the overall process. Since work is associated with the change of Hamiltonian $H_S(t)$ of the system, we only need to couple the system to the detector before and after the variation of Hamiltonian $H_S(t_{n-1}) \to H_S(t_n)$ to obtain the work produced from t_{n-1} and t_n. And, the evolution of the system-environment-detector (S-E-D) whole system is described by the operator (see Fig. 2)

$$
\mathcal{U}_{\chi, W} = \mathcal{U}_{\chi, W}^N \ldots \mathcal{U}_{\chi, W}^2 \mathcal{U}_{\chi, W}^1,
\tag{21}
$$

with

$$
\begin{aligned}
\mathcal{U}_{\chi, W}^n &= U_{\chi, t_n} U_{t_{n-1}}^{t_n} U_{-\chi, t_{n-1}} U_{E_n E_{n+1}} U_{SE_n} \; (1 \leqslant n < N), \\
\mathcal{U}_{\chi, W}^n &= U_{\chi, t_n} U_{t_{n-1}}^{t_n} U_{-\chi, t_{n-1}} U_{SE_n} \; (n = N),
\end{aligned}
\tag{22}
$$

where $U_{\chi, t_n} = \exp[i\chi H_S(t_n) \bigotimes H_D]$ and $U_{-\chi, t_{n-1}} = \exp[-i\chi H_S(t_{n-1}) \bigotimes H_D]$. In order to decompose the evolution process of the dynamics, at t_n, the time-dependent eigenstates of the system can be denoted by $\{|i_n\rangle\}$, $\{|j_n\rangle\}$, $\{|k_n\rangle\}$, and $\{|l_n\rangle\}$. For the nth ancilla $(1 < n < N)$, we denote the Hamiltonian eigenbasis after the interaction between the $(n-1)$th ancilla and nth ancilla as $\{|f_n^1\rangle\}$ and $\{|h_n^1\rangle\}$, the Hamiltonian eigenbasis after the interaction between the nth ancilla and the system as $\{|f_n^2\rangle\}$ and $\{|h_n^2\rangle\}$, and the Hamiltonian eigenbasis after the interaction between the nth ancilla and the $(n+1)$th ancilla as $\{|f_n^3\rangle\}$ and $\{|h_n^3\rangle\}$. For $n = 1$, there is no interaction with the previous ancilla, while for the Nth ancilla, there is no interaction with the following ancilla. Based on Eq. (18), the QCGF of work can

be calculated (see Appendix)

$$\mathcal{G}_{\chi,\mathcal{W}} = \sum_{P_1,P_2} e^{i\frac{\chi}{2}\lambda\left(w_{P_1}^N + w_{P_2}^N\right)} \Lambda_{i_N f_N^2, i_0 f_1}^{P_1}$$

$$\times \rho_{i_0,j_0} \rho_{f_1,h_1} \cdots \rho_{f_N,h_N} \left(\Lambda_{j_0 h_1, j_N h_N^2}^{P_2}\right)^\dagger, \qquad (23)$$

where P_1 and P_2 represent the transition paths of the system and environment, $\Lambda_{i_N f_N^2, i_0 f_1}^{P_1}$ is the probability amplitude of the transition path P_1: $|i_0, f_1, f_2, \ldots, f_N\rangle \to |i_N, f_1^2, f_2^3, \ldots, f_N^2\rangle$, and $(\Lambda_{j_0 h_1, j_N h_N^2}^{P_2})^\dagger$ is the probability amplitude from $|j_0, h_1, h_2, \ldots, h_N\rangle$ to $|j_N, h_1^2, h_2^3, \ldots, h_N^2\rangle$ (see Appendix for more details). Along the paths P_1 and P_2, the work done on the system is $w_{P_1}^N = \sum_{n=1}^{N} \varepsilon_{i_n} - \varepsilon_{k_{n-1}}$ and $w_{P_2}^N = \sum_{n=1}^{N} \varepsilon_{j_n} - \varepsilon_{l_{n-1}}$, respectively. Then, the work QPDF is obtained by taking the Fourier transformation

$$\mathcal{P}(W) = \sum_{P_1,P_2} \Lambda_{i_N f_N^2, i_0 f_1}^{P_1} \rho_{i_0,j_0} \rho_{f_1,h_1} \cdots \rho_{f_N,h_N} \left(\Lambda_{j_0 h_1, j_N h_N^2}^{P_2}\right)^\dagger$$

$$\times \delta\left[W - \frac{\lambda}{2}\left(w_{P_1}^N + w_{P_2}^N\right)\right]. \qquad (24)$$

Also, the environment degrees of freedom is traced out in Eq. (23), thus $f_n^2 = h_n^2$ for $n = 1, N$, and $f_n^3 = h_n^3$ for $1 < n < N$. We emphasize here that there is no difference whether we trace out the nth ancilla immediately after the interaction between the nth ancilla and the $(n+1)$th ancilla, or trace out the ancilla at the end of the evolution in both paths P_1 and P_2. Since the degree of freedom of the system is traced out after the last evolution in the paths P_1 and P_2, $j_N = i_N$ is satisfied.

B. QPDF of heat

In analogy to work, heat is also not a state function which depends on the path swept by the system in the evolution process. In addition, the heat absorbed by the system is entirely due to the interaction between the system and the environment. To obtain the energy exchange between the system and the nth ancilla, we turn on the system-detector coupling before the interaction between the system and the nth ancilla and after the interaction between the nth ancilla and the $(n+1)$th ancilla (see Fig. 2). Thus, the evolution operator of S-E-D from 0 to t_N can be written as

$$\mathcal{U}_{\chi,Q} = \mathcal{U}_{\chi,Q}^N \cdots \mathcal{U}_{\chi,Q}^2 \mathcal{U}_{\chi,Q}^1, \qquad (25)$$

with

$$\mathcal{U}_{\chi,Q}^n = U_{t_{n-1}}^{t_n} U_{-\chi,t_n} U_{E_n E_{n+1}} U_{SE_n} U_{\chi,t_n} \ (1 \leqslant n < N),$$

$$\mathcal{U}_{\chi,Q}^n = U_{t_{n-1}}^{t_n} U_{-\chi,t_n} U_{SE_n} U_{\chi,t_n} \ (n = N), \qquad (26)$$

Similar to the derivation of the QPDF of work, the final density operator of the system and the detector after N steps reads

$$\rho_N = \sum_{P_1,P_2} \rho_{\lambda,\lambda'} e^{i\frac{\chi}{2}\left(\lambda q_{P_1}^N - \lambda' q_{P_2}^N\right)} \Lambda_{i_N f_N^2, i_0 f_1}^{P_1}$$

$$\times \rho_{i_0,j_0} \rho_{f_1,h_1} \cdots \rho_{f_N,h_N} \left(\Lambda_{j_0 h_1, j_N h_N^2}^{P_2}\right)^\dagger$$

$$\times |i_N, \lambda\rangle\langle j_N, \lambda'|, \qquad (27)$$

where the heat flowing from the system to the environment is $q_{P_1}^N = \sum_{n=1}^{N} \varepsilon_{k_{n-1}} - \varepsilon_{i_{n-1}}$ and $q_{P_2}^N = \sum_{n=1}^{N} \varepsilon_{l_{n-1}} - \varepsilon_{j_{n-1}}$ along paths P_1 and P_2, respectively. The QPDF of heat is

$$\mathcal{P}(Q) = \sum_{P_1,P_2} \Lambda_{i_N f_N^2, i_0 f_1}^{P_1} \rho_{i_0,j_0} \rho_{f_1,h_1} \cdots \rho_{f_N,h_N} \left(\Lambda_{j_0 h_1, j_N h_N^2}^{P_2}\right)^\dagger$$

$$\times \delta\left[Q - \frac{\lambda}{2}\left(q_{P_1}^N + q_{P_2}^N\right)\right]. \qquad (28)$$

C. QPDF of the variation of internal energy

Now we concentrate on the QPDF of variation of internal energy. Unlike work and heat, internal energy is a state function, so the change of internal energy only depends on the initial and the final state of the system. As shown in Fig. 2, we only need to couple the system and detector at the beginning t_0 and at the end of the evolution t_N, which generates the S-E-D evolution

$$\mathcal{U}_{\chi,\Delta U} = U_{\chi,t_N} U_N \cdots U_1 U_{-\chi,t_0}. \qquad (29)$$

After N interactions between the system and ancilla, the final density operator of the system and the detector reads

$$\rho_N = \sum_{P_1,P_2} \rho_{\lambda,\lambda'} e^{i\frac{\chi}{2}[\lambda(i_N - i_0) - \lambda'(j_N - j_0)]} \Lambda_{i_N f_N^2, i_0 f_1}^{P_1}$$

$$\times \rho_{i_0,j_0} \rho_{f_1,h_1} \cdots \rho_{f_N,h_N} \left(\Lambda_{j_0 h_1, j_N h_N^2}^{P_2}\right)^\dagger$$

$$\times |i_N, \lambda\rangle\langle j_N, \lambda'|. \qquad (30)$$

Based on Eqs. (18) and (20), the QPDF of the variation of internal energy can be written as

$$\mathcal{P}(\Delta U) = \sum_{P_1,P_2} \Lambda_{i_N f_N^2, i_0 f_1}^{P_1} \rho_{i_0,j_0} \rho_{f_1,h_1} \cdots \rho_{f_N,h_N} \left(\Lambda_{j_0 h_1, i_N h_N^2}^{P_2}\right)^\dagger$$

$$\times \delta\left(\Delta U - \frac{\lambda}{2}[(i_N - i_0) + (i_N - j_0)]\right). \qquad (31)$$

IV. RESULTS

Based on Eqs. (24), (28), and (31), we investigate the QPDFs of work, heat, and the variation of internal energy in Markovian and non-Maokovian dynamics. In this section, we specifically consider the initial state of the system as $|\psi_{S_0}\rangle = \cos(\theta)|g_0\rangle + \sin(\theta)|e_0\rangle$, with $\theta = \pi/4$. All the ancillas are initialized in the same equilibrium state $\rho_{E_n} = e^{-\beta_E E_g}/Z_E |g\rangle\langle g| + e^{-\beta_E E_e}/Z_E |e\rangle\langle e|$, where $\beta_E = \frac{1}{T}$ is the inverse temperature of the environment and the partition function $Z_E = \text{Tr}[e^{-\beta_E H_{E_n}}]$. In this paper, we assume $\omega t_N = \pi$, then $\|\Delta H_S\| = 1/2$.

A. Markovian environment

In this section, we concentrate on the Markovian environment, i.e., there is no interaction between ancillas ($\Gamma = 0$). The probability distributions of work, heat, and the variation of internal energy for the TPM and the QPDF with different environmental temperatures $\ln T = -3, 1, 5$ are plotted in Fig. 3. In classical dynamics, there is no energy exchange at half of the energy gap of the system and the probability is always positive. But, when quantum effects such as quantum coherence of the initial state and quantum interference effects
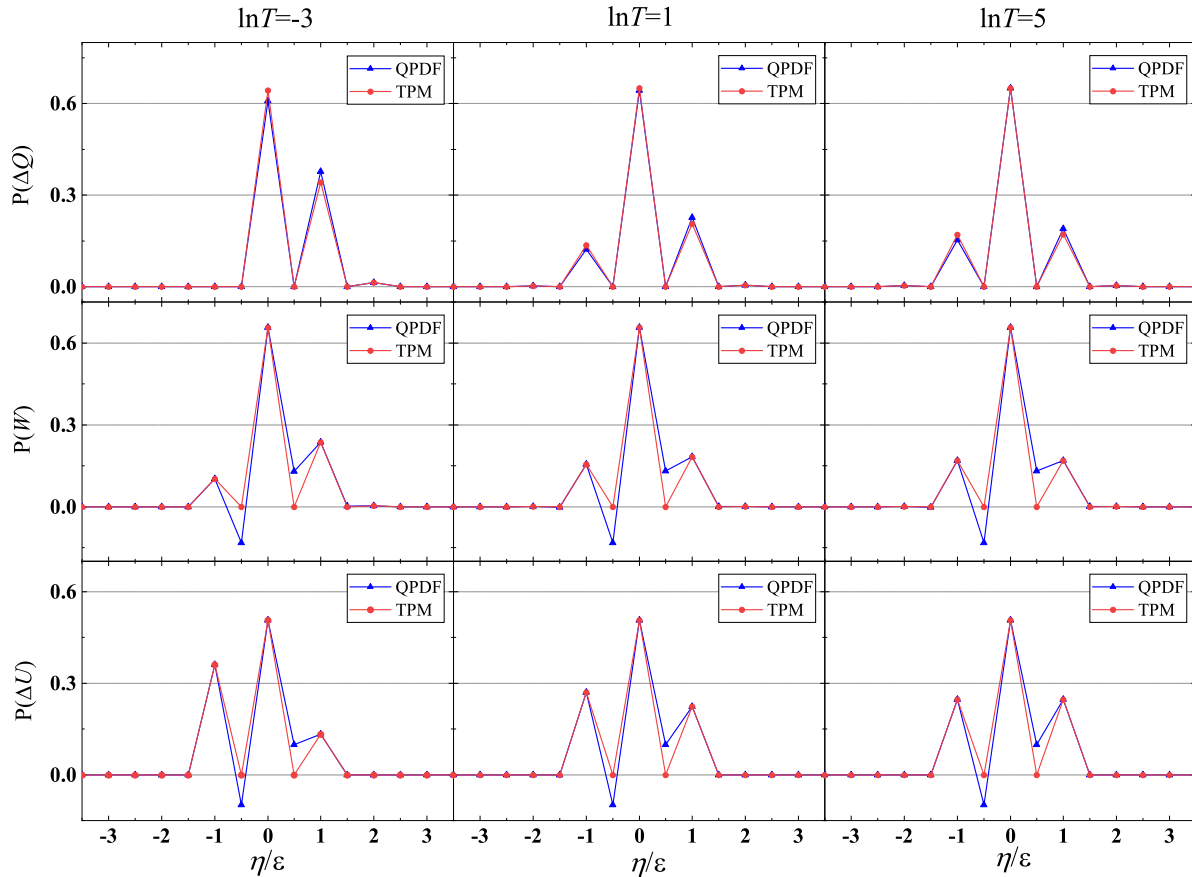
FIG. 3. The QPDFs (blue triangle) and the probability distributions for the TPM (red solid circle) of heat, work, and the variation of internal energy for different environmental temperatures $\ln T = -3, 1, 5$. η represents ΔQ in the first row, W in the second row, and ΔU in the third row, and the other parameters are $N = 5$, $\Lambda = 0.3\pi/2$, and $g = 0.5\omega$.

appear, there will be negative quasiprobabilities at half of the energy gap of the system. It can be seen from Fig. 3 that for the QPDFs of work and the variation of internal energy, the negative quasiprobabilities and the nonzero quasiprobabilities at $\eta/\varepsilon = \pm 1/2$ appear, where η can be W, ΔQ, or ΔU introduced in Eq. (18). For the TPM, the probabilities of work and the variation of internal energy at $\eta/\varepsilon = \pm 1/2$ are equal to 0, there is no energy exchange at half of the energy gap of the system, and the probability density distributions are always positive. However, for the exchange of whole energy quantum, the QPDFs of work and the variation of internal energy are the same as that obtained in the TPM. We also find that unlike the QPDFs of the work and the variation of internal energy, the QPDF of the heat at half of the energy gap of the system is always 0, and there is no negative value in the QPDF of heat. This is because heat carries the classical energy exchange with the environment. Although there are no negative QPDFs of heat at half of the energy gap of the system, the QPDF of heat at the whole energy quantum is different from that obtained by the TPM. In addition, we find that variation of internal energy is within ± 1, while the variations of the heat and work are not limited by $\eta/\varepsilon = \pm 1$. This is because the internal energy only measures the energy variation of the initial and final states of the system, while heat and work track the energy change of the system throughout the whole process, allowing for a wider range of energy distribution.

In order to describe the effect of the environmental temperature on the quantumness of rhe dynamic system quantitatively, a new quantity $\mathcal{Q}(\eta)$ [65,66] is introduced and defined as

$$\mathcal{Q}(\eta) = -1 + \sum_{\eta} |\mathcal{P}(\eta)|, \qquad (32)$$

where $|\bullet|$ represents the absolute value of $\bullet$, and η might be W, ΔQ, or ΔU. When $\{\mathcal{P}(\eta)\}$ is nonnegative, $\mathcal{Q}(\eta) = 0$. If there exists the probability $\mathcal{P}(\eta) < 0$, then $\mathcal{Q}(\eta) > 0$. $\mathcal{Q}(W)$ and $\mathcal{Q}(\Delta U)$ for the QPDF as functions of environmental temperature are plotted in Fig. 4. It can be seen that with the change of environmental temperature, both $\mathcal{Q}(W)$ and $\mathcal{Q}(\Delta U)$ remain almost unchanged, indicating that the environmental temperature has little effect on the quantumness of the system. This indicates that the environmental temperature does not affect the decoherence process induced by interacting with the environment. Moreover, the expected values of W, ΔQ, and ΔU are plotted as functions of $\ln T$ in Fig. 5. It shows that W and ΔQ decrease with the increase of environmental temperature, while ΔU increase with the environmental temperature in both TPM and QPDF. In other words, as the environmental temperature increase, the heat flowing from the system to environment decreases, the work done on the system decreases, and the variation of internal energy increases. As the environmental temperature
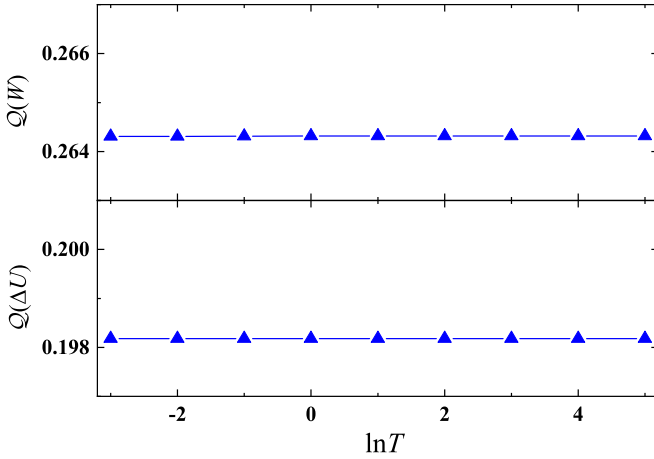
FIG. 4. $\mathcal{Q}(W)$ and $\mathcal{Q}(\Delta U)$ for the QPDF as functions of the environmental temperature $\ln T$. The other parameters are the same as that in Fig. 3.

increases, the energy absorbed by the environment from the system decreases, leading to an increase in the internal energy of the system. Consequently, the probability of the system being excited to a higher energy level under external driving decreases, leading to a decrease in the average work done by the external driving on the system. Moreover, it is evident from Fig. 5 that the QPDF preserves the initial coherence of the system, and the average values of work and heat absorbed by the system are both higher than the results obtained by TPM. Thus, it is confirmed that quantum coherence can be considered an energy resource in extraction of energy.

In the following, we discuss the effect of evolution speed on the probability distributions of work, heat, and variation of internal energy. In Fig. 6, we plot the QPDFs and the probability distributions for the TPM of work, heat, and the variation of internal energy with different interaction times $N = 5, 15, 100$. The corresponding evolution speed $v = \|\Delta H_S\|/N = 1/10, 1/30, 1/200$, where $\|\Delta H_S\| = 1/2$ represents the norm of the variation of the system Hamiltonian
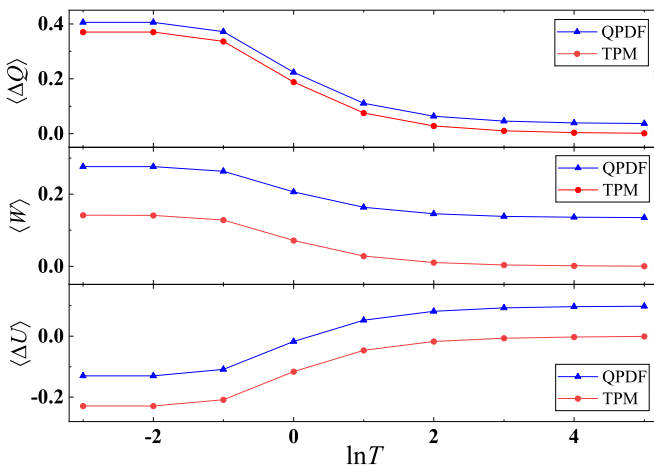

FIG. 5. The average values of heat, work, and the variation of internal energy as functions of the environmental temperature $\ln T$. The other parameters are the same as Fig. 3.

between $H_S(0)$ and $H_S(t_N)$. It can be seen from Fig. 6 that, compared with $N = 15$ and $N = 100$, when the system is driven quickly ($N = 5$), the magnitudes of the probability of work and variation of internal energy at $\eta/\varepsilon = \pm 1/2$ are the largest, which indicates that the quantumness of the system is the strongest at $N = 5$. For $N = 15$, we find that compared with $N = 5$, the amplitudes of the quasiprobability of work and the variation of internal energy at half of the energy gap of the system become smaller. Moreover, when comparing the results for the QPDF and the TPM, we find that for work, heat, and the variation of internal energy, as the evolution speed slows down the QPDFs and the probability distributions for the TPM are getting closer. For $N = 100$, we find that the QPDFs of work, heat, and the variation of internal energy almost coincides with the probability distribution obtained by the TPM. This is well illustrated by $\mathcal{Q}(W)$ and $\mathcal{Q}(\Delta U)$ in Fig. 7, which shows that with the increasing of the collision times N, i.e., the slowing down of the evolution speed, $\mathcal{Q}(W)$ and $\mathcal{Q}(\Delta U)$ decrease. When the driving speed is slow enough ($N \gg 1$), both $\mathcal{Q}(W)$ and $\mathcal{Q}(\Delta U)$ are close to 0, and the results of QPDF coincide with the results of TPM. This is because when the Hamiltonian $H_S(t)$ of the system varies sufficiently slowly, the adiabatic limit is reached, which means that the instantaneous eigenstate at one time evolves continuously to the corresponding eigenstate at later times, and will not transfer to other energy levels. In other words, its population in each level remains unchanged. Thus, the quantumness of the dynamics disappears and the classical limit is reached.

Next we focus on the effect of S-E interaction on the probability distributions of work, heat, and the variation of internal energy. The probability distributions of ΔQ, W, and ΔU for the QPDF and TPM for different S-E coupling strengths are shown in Fig. 8. For $\Lambda = 0$, i.e., the system is isolated, there is no interaction between the system and the environment, and the system is only subject to the drive by Hamiltonian $H_S(t)$. In this case, $\mathcal{Q}(W)$ and $\mathcal{Q}(\Delta U)$ are the largest, which indicates that the quantumness of the system is the strongest. Notably, there is no heat exchange between the system and the environment, so the probability distribution of the heat only concentrates on $\Delta Q = 0$. For both the QPDF and the TPM, the probability distributions of work are identical to the probability distributions of the variation of internal energy exactly. When the S-E coupling strength $\Lambda = \pi/4$, the absolute values of the quasiprobability of work and the variation of internal energy at half of the energy gap of the system decrease compared with $\Lambda = 0$. When the system and the environment are completely swapped ($\Lambda = \pi/2$), the quasiprobabilities of W and ΔU at $\eta/\varepsilon = \pm 1/2$ are 0. In this case, the quantumness completely disappears. Because every S-E interaction means a complete exchange between the states of the system and the ancilla, the initial state of the system is reset to the thermal state, thus the initial quantum coherence of the system is completely destroyed. The above statement is shown by $\mathcal{Q}(W)$ and $\mathcal{Q}(\Delta U)$ for the QPDF (see Fig. 9). For an isolated system ($\Lambda = 0$), the values of $\mathcal{Q}(W)$ and $\mathcal{Q}(\Delta U)$ are the largest, i.e., the quantumness of the system is the strongest. It can be concluded that the S-E coupling weakens the quantumness of the system. Furthermore, when the S-E coupling is the strongest ($\Lambda = \pi/2$), the dissipation destroys the initial coherence of the system completely.
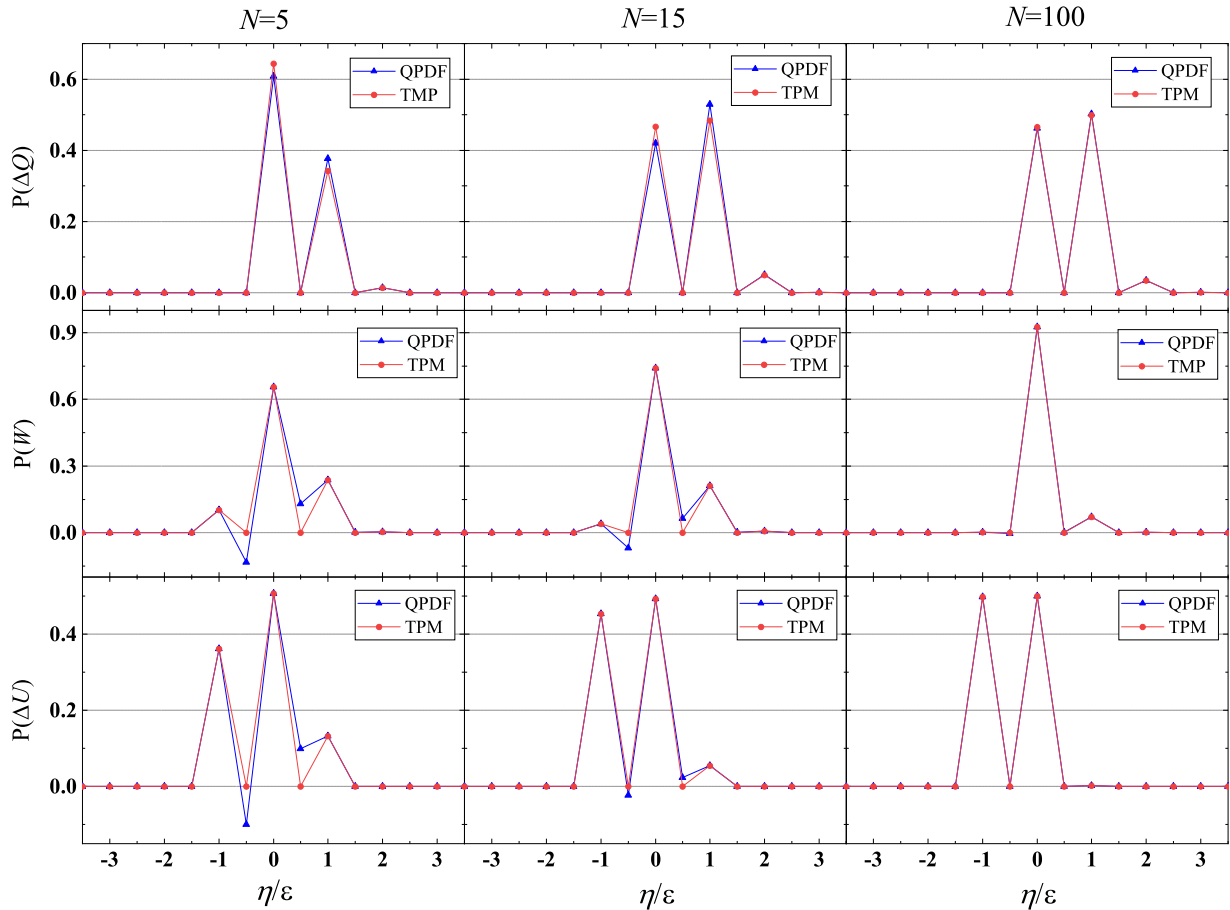
FIG. 6. The QPDFs (blue triangle) and the probability density distributions for the TPM (red solid circle) of heat, work, and the variation of internal energy for different driving speed $v = 1/10, 1/30, 1/200$, with $\ln T = -3$, $\Lambda = 0.3\pi/2$, and $g = 0.5\omega$.

B. Non-Markovian environment

In the above section, we have discussed the QPDFs of work, heat, and the variation of internal energy in Markovian dynamics. In this section we focus on the effect of non-Markovianity on the QPDFs of work, heat, and variation of
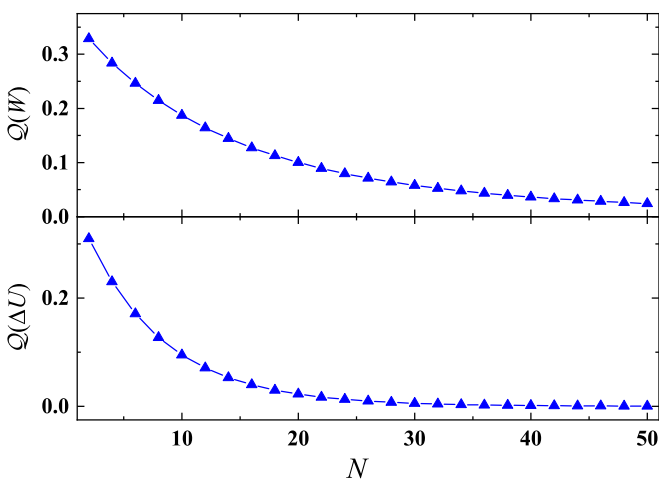
FIG. 7. $\mathcal{Q}(W)$ and $\mathcal{Q}(\Delta U)$ for the QPDF as functions of collision time N, and the other parameters are the same as that in Fig. 6.

internal energy. It has been shown above that the memory is introduced by the interaction between ancillas [60]. In this section, we consider the nonzero coupling strengths between ancillas. In Fig. 10, we plot the QPDFs and the probability distributions for the TPM of W, ΔQ, and ΔU under two environment temperatures $\ln T = -3$ and $\ln T = 5$ with $\Gamma = 0.5\pi/2$. As shown in Fig. 10, similar to Markovian dynamics, we observe that there are no negative quasiprobabilities at half of the energy gap for QPDF of ΔQ even when $\Gamma \neq 0$. In order to quantitatively describe how the quantumness of the system changes with the environmental temperature in non-Markovian dynamics, $\mathcal{Q}(W)$ and $\mathcal{Q}(\Delta U)$ are plotted as functions of the environmental temperature $\ln T$ in Fig. 11. We find that as the environmental temperature increases, $\mathcal{Q}(W)$ and $\mathcal{Q}(\Delta U)$ become small, which shows that the lower the environmental temperature, the stronger the quantumness of the system, and the higher the temperature, the weaker the quantumness of the system. In addition, we have shown that in the Markovian regime, the influence of temperature on the quantumness is negligible, but when interaction between ancillas is introduced, the influence of the temperature on the quantumness is obvious.

In order to make it clearer whether the variation in quantumness is caused by change of the degree of non-Markovianity, we introduce a measurement of non-Markovianity based on the dynamics of the trace distance
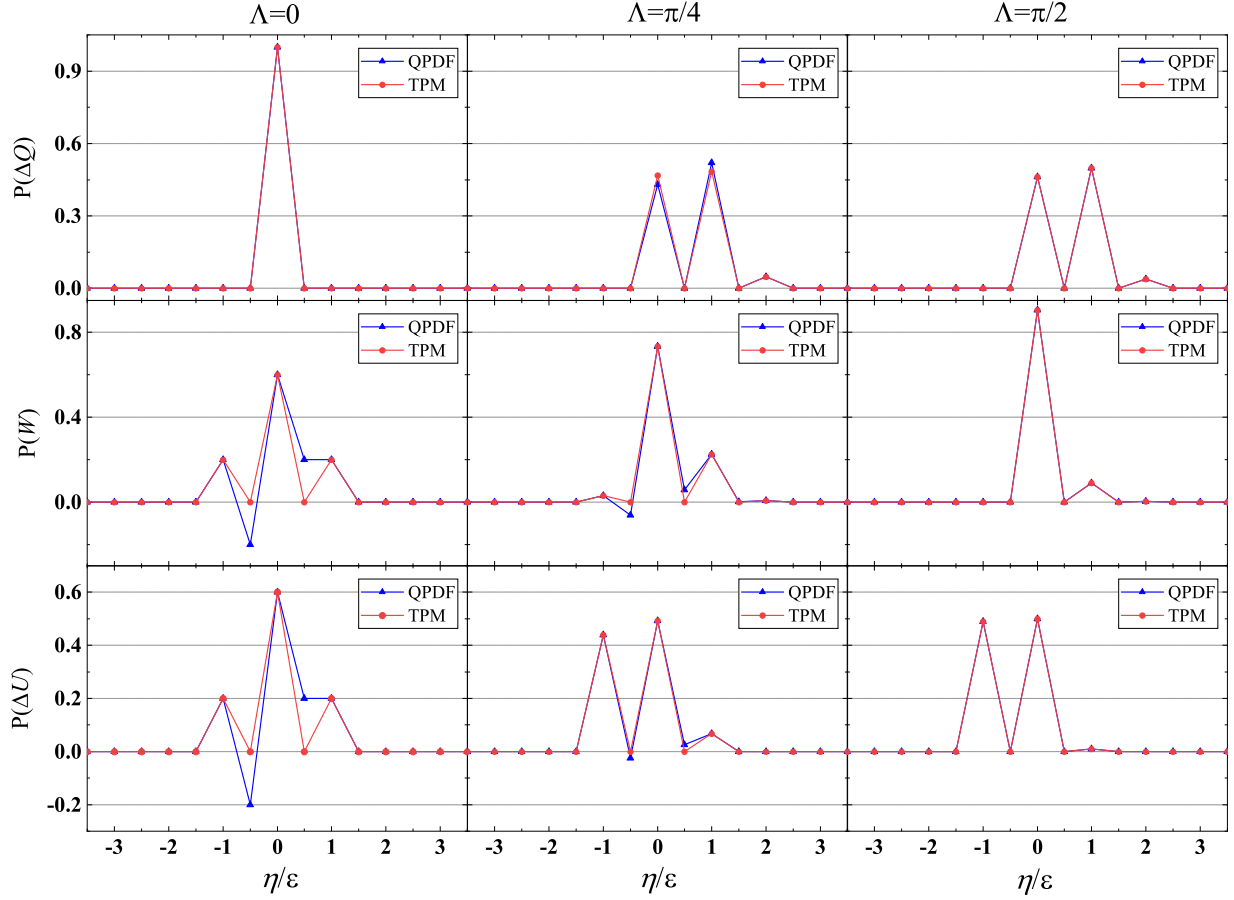
FIG. 8. The QPDFs (blue triangle) and the probability density distributions for the TPM (red solid circle) of heat, work, and the variation of internal energy for different S-E coupling strengths $\Lambda = 0, \pi/4, \pi/2$. The other parameters are $\ln T = -3$, $N = 5$, and $g = 0.5\omega$.

[67]. The trace distance for two quantum states ρ_1 and ρ_2 is defined as

$$D(\rho_1, \rho_2) = \tfrac{1}{2}\mathrm{tr}|\rho_1 - \rho_2|, \tag{33}$$

where $|A| = \sqrt{A^\dagger A}$. The trace distance D can be used as a measure of the distinguishability of any two quantum states,
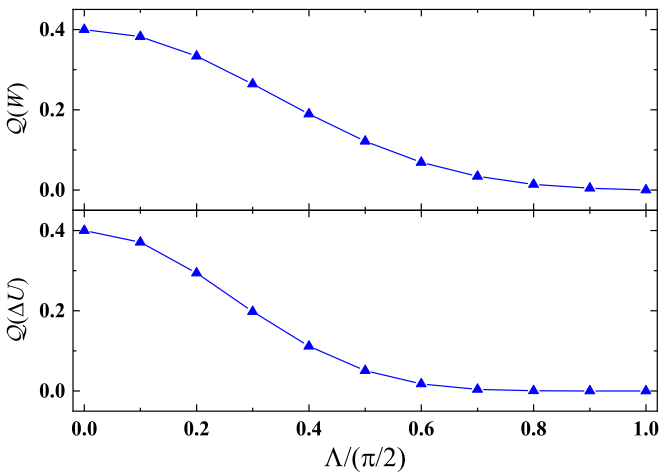
$D(\rho_1, \rho_2) = 1$ for two completely distinguishable states ρ_1 and ρ_2 and $D(\rho_1, \rho_2) = 0$ for identical states. If ρ_{1,S_n} and ρ_{2,S_n} are the system states obtained after n sequence mappings, with the initial system state being ρ_{1,S_0} and ρ_{2,S_0}, respectively, the
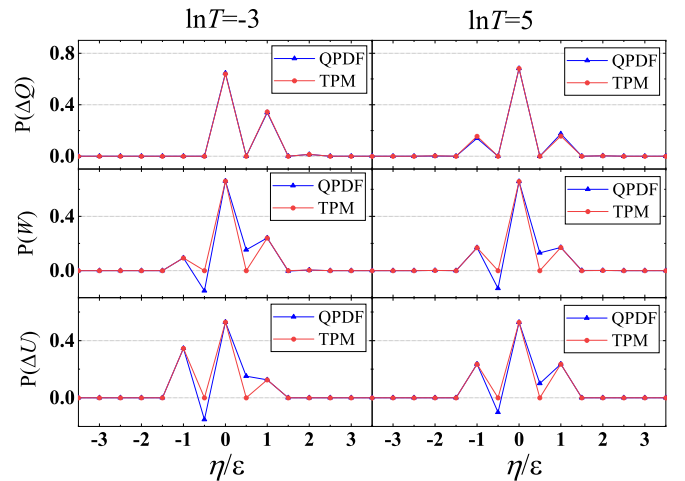

FIG. 9. $\mathcal{Q}(W)$ and $\mathcal{Q}(\Delta U)$ for the QPDF as functions of S-E coupling strength Λ. The other parameters are the same as those in Fig. 8.

FIG. 10. The QPDFs (blue triangle) and the probability distributions for the TPM (red solid circle) of the ΔQ, W, and ΔU at low environmental temperature ($\ln T = -3$) and high environmental temperature ($\ln T = 5$). The other parameters are $g = 0.5\omega$, $N = 5$, $\Lambda = 0.3\pi/2$, and $\Gamma = 0.5\pi/2$.
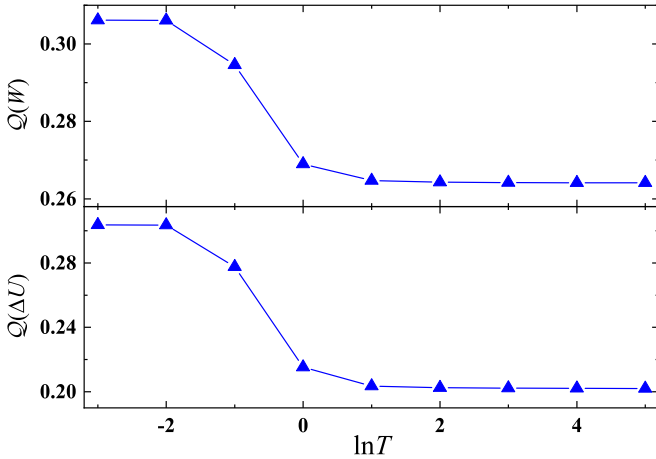
FIG. 11. $\mathcal{Q}(W)$ and $\mathcal{Q}(\Delta U)$ for the QPDF as functions of the environmental temperature $\ln T$. The other parameters are the same as in Fig. 10.

degree of non-Markovianity can be written as

$$\mathcal{N} = \max \sum_n \left[D\left(\rho_{1,S_n}, \rho_{2,S_n}\right) - D\left(\rho_{1,S_{n-1}}, \rho_{2,S_{n-1}}\right) \right], \quad (34)$$

where $\mathcal{N}$ accounts for the contribution of all intervals where the trace distance between any pair of initial states increase, and "max" represents the maximization over all possible pairs of the initial state of the system. In general, the maximum only occurs in these two pairs of states: $(|g(0)\rangle + |e(0)\rangle)/\sqrt{2}$, $(|g(0)\rangle - |e(0)\rangle)/\sqrt{2}$ or $|g(0)\rangle, |e(0)\rangle$ [60,68]. From numerical calculations, we find that for the collision model used in this paper, the degree of non-Markovianity of Eq. (34) obtained for the pair of initial state $(|g(0)\rangle + |e(0)\rangle)/\sqrt{2}$, $(|g(0)\rangle - |e(0)\rangle)/\sqrt{2}$ is larger than that obtained for $|g(0)\rangle, |e(0)\rangle$. In Fig. 12, we present the degree of non-Markovianity $\mathcal{N}$ as a function of the environmental temperature $\ln T$ with the pair of initial system states $(|g(0)\rangle + |e(0)\rangle)/\sqrt{2}$, $(|g(0)\rangle - |e(0)\rangle)/\sqrt{2}$ at AA coupling
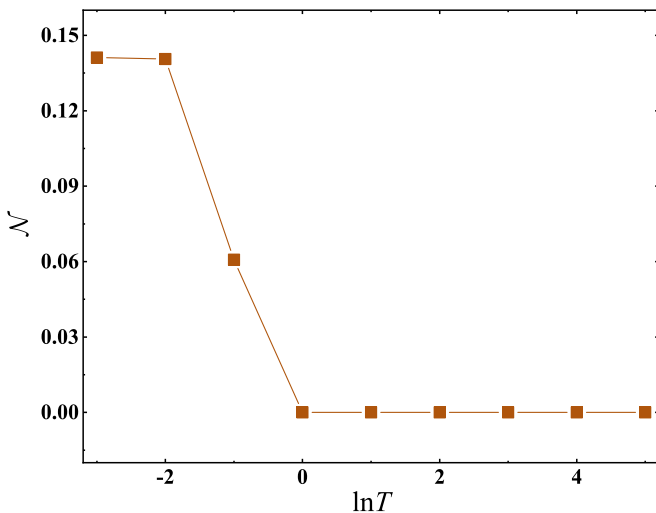

FIG. 12. The degree of non-Markovianity $\mathcal{N}$ as a function of the environmental temperature $\ln T$, with $g = 0.5\omega$, $v = 1/10$, $n = 1000$, $\Lambda = 0.3\pi/2$, and $\Gamma = 0.5\pi/2$.
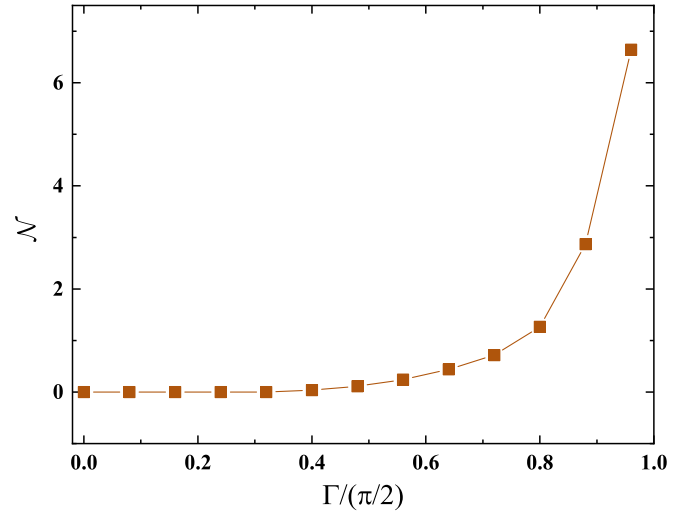

FIG. 13. The degree of non-Markovianity $\mathcal{N}$ as a function of the AA coupling strength Γ, $g = 0.5\omega$, $v = 1/10$, $n = 1000$, $\Lambda = 0.3\pi/2$, and $\ln T = -3$.

strength $\Gamma = 0.5\pi/2$. Through our study, we find that the degree of non-Markovianity of the dynamics depends not only on the coupling strength between ancillas, but also on the environmental temperature. When the environment is at low temperature, the degree of non-Markovianity is relatively large. As the temperature increases, the degree of non-Markovianity decreases. And, when the environmental temperature reaches a certain temperature, the dynamics of the system is almost Markovian. When the environmental temperature is high, it is approximately in a maximally mixed state and contains the richest information. In addition, the interaction between the environment and the system has little effect on the environment, resulting in little information flowing back from the environment to the system, so the dynamics process is almost Markovian. Conversely, at low environmental temperature, the information flowing from the system to the environment will flow back into the system, leading to non-Markovian dynamics.

Above we have discussed the influence of temperature on the degree of non-Markovianity and the QPDFs of work, heat, and the variation of internal energy, and we find that at high environmental temperature, the degree of non-Markovianity is almost 0, i.e., the dynamics is Markovian. Thus, in the following, we concentrate on low environmental temperature to study the effect of the degree of non-Markovianity on the probability distributions of work, heat, and the variation of internal energy. In Fig. 13, we show the degree of non-Markovianity $\mathcal{N}$ as a function of the coupling strength between the ancillas at low environmental temperature $\ln T = -3$. It is important to note that even when $\Gamma \neq 0$, the dynamics may still be Markovian. This is because the memory effect is only activated if the AA coupling exceeds a certain threshold [69]. From Fig. 13, we can find that in the interval $0 \leqslant \Gamma \leqslant \frac{\pi}{2}$, $\mathcal{N}$ increases with Γ, thus the AA coupling strength Γ can be considered as a measure of non-Markovianity.

In Fig. 14, the QPDFs of work, heat, and the variation of internal energy and the probability distributions for the TPM for different AA coupling strengths are plotted. When
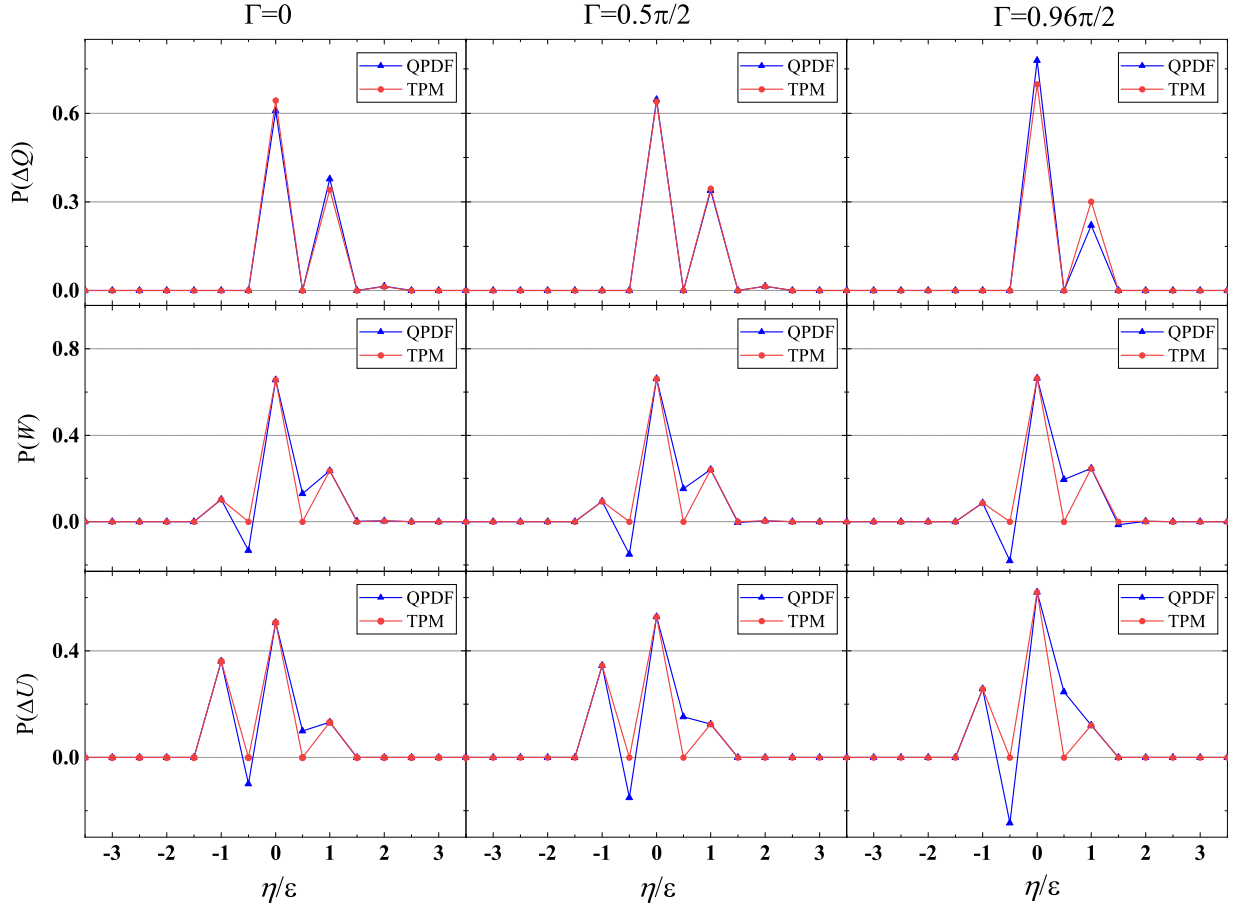
FIG. 14. The QPDFs (blue triangle) and the probability density distributions for the TPM (red solid circle) of heat, work, and the variation of internal energy for different AA coupling strengths $\Gamma = 0, 0.5\pi/2, 0.96\pi/2$. The other parameters are $g = 0.5\omega$, $N = 5$, $\Lambda = 0.3\pi/2$, and $\ln T = -3$.

the coupling strength between ancillas $\Gamma = 0$, the dynamics is Markovian. When the AA coupling strength is $0.5\pi/2$, we find that compared to the Markovian dynamics, the magnitudes of the quasiprobability of the work and the variation of internal energy at half of the energy gap increase, i.e., the quantumness of the system is enhanced. For $\Gamma = 0.96\pi/2$, the magnitudes of the quasiprobabilities of W and ΔU at $\eta/\varepsilon = \pm 1/2$ are larger than those obtained for $\Gamma = 0.5\pi/2$. The quantumness of the system for $\Gamma = 0.96\pi/2$ is stronger than that for $\Gamma = 0.5\pi/2$. In Fig. 15, $\mathcal{Q}(W)$ and $\mathcal{Q}(\Delta U)$ are plotted to show the dependence of quantumness on the coupling strength between ancillas. It can be seen from Fig. 15 that $\mathcal{Q}(W)$ and $\mathcal{Q}(\Delta U)$ increase as the AA coupling strength Γ increases, i.e., the stronger the coupling between ancillas, the stronger the quantumness of the dynamics. This is because, due to the memory effect, information about the initial coherence of the system that flows to the environment returns to the system, and the stronger the memory effect, the more information flows back to the system, and the stronger the quantumness.

V. CONCLUSION

In this paper we studied the QPDFs and probability distributions for the TPM of work, heat, and the variation of

internal energy for a driven open quantum system. When the initial system state is incoherent, the QPDFs and probability distributions for the TPM of work, heat, and the variation of internal energy are consistent. But, for the system state with initial coherence, the QPDFs of work and the variation of
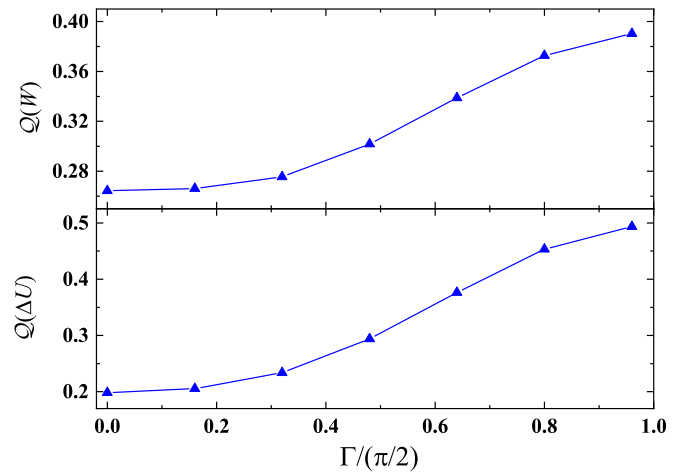

FIG. 15. $\mathcal{Q}(W)$ and $\mathcal{Q}(\Delta U)$ for the QPDF as functions of AA coupling strengths Γ. The other parameters are the same as in Fig. 14.

internal energy might be negative at half of the energy gap of the system, while the probability distributions for the TPM is always positive. And, the negative QPDF can be regarded as the witness of quantumness.

In the Markovian regime, we found that the temperature of the environment has little effect on the quantumness of the dynamics, but the average values of work and heat decrease and the average value of the variation of internal energy increases as the temperature increases. As the driving speed slows down, the quantumness of the system is weakened. When the driving speed is slow enough, i.e., when the variation of the system Hamiltonian is sufficiently slow, the condition of the adiabatic approximation is reached. Therefore, the quantumness of the system disappears and the system reaches the classical limit. In this case, the QPDFs are consistent with the results obtained by the TPM. And, as the coupling strength between the system and the environment increases, the quantumness of the system is also weakened.

When the coupling strength between ancillas $\Gamma \neq 0$, the memory effect is introduced. We found that in contrast to high environmental temperature, low temperature results in larger $\mathcal{Q}(W)$ and $\mathcal{Q}(\Delta U)$. This indicates that decreasing the environmental temperature enhances the quantumness of the system. We found that when the environmental temperature is high, the degree of non-Markovianity is almost 0. The lower the environmental temperature, the larger the degree of non-Markovianity. Thus, the change of quantumness of the system is mainly caused by the variation of non-Markovianity. In

addition, we found that the stronger the coupling between ancillas, the stronger the non-Markovianity. When the coupling between ancillas is enhanced, the quantumness of the system is enhanced. Therefore, as the degree of non-Markovianity is increased, the quantumness of the system is enhanced. In fact, we demonstrated that non-Markovianity can serve as an energy resource for extracting energy from thermal reservoirs and enhancing the power output, representing a significant advancement for the future application of memory effect in quantum heat engines.

APPENDIX: DETAILED DERIVATION OF THE QPDF OF WORK

To derive Eqs. (23) and (24) in the main text, i.e., the QCGF and the QPDF of work introduced in Sec. II A, we start from Eq. (21). The operator sequence Eq. (21) consisting of the interaction between the system and ancilla U_{SE_1}, the interaction between E_1 and E_2, first system-detector coupling $U_{-\chi,0}$, system evolution $U_0^{t_1}$, and second system-detector coupling U_{χ,t_1} leads to the evolution

$$
\begin{aligned}
\rho_0 \rightarrow &\sum \rho_{f_1h_1}\rho_{f_2h_2}\cdots\rho_{f_Nh_N}\rho_{\lambda,\lambda'}\left(U_{SE_1}\right)_{k_0f_1^1,i_0f_1}\rho_{i_0,j_0}\left(U_{SE_1}\right)^\dagger_{j_0h_1,l_1h_1^1}\left|k_0,f_1^1,f_2,...,f_N,\lambda\right\rangle\left\langle l_0,h_1^1,h_2,...,h_N,\lambda'\right| \\
\rightarrow &\sum \rho_{f_1,h_1}\rho_{f_2h_2}\cdots\rho_{f_Nh_N}\rho_{\lambda,\lambda'}\left(U_{E_1E_2}\right)_{f_2^2f_1^1,f_1^1f_2}\left(U_{SE_1}\right)_{k_0f_1^1,i_0f_1}\rho_{i_0,j_0}\left(U_{SE_1}\right)^\dagger_{j_0h_1,l_1h_1^1}\left(U_{E_1E_2}\right)^\dagger_{h_1^1h_2,h_1^2h_2^1} \\
&\times \left|k_0,f_1^2,f_2^1,...,f_N,\lambda\right\rangle\left\langle l_0,h_1^2,h_2^1,...,h_N,\lambda'\right| \\
\rightarrow &\sum \rho_{f_1,h_1}\rho_{f_2h_2}\cdots\rho_{f_N,h_N}\rho_{\lambda,\lambda'}e^{i\frac{\chi}{2}(\lambda\varepsilon_{k_0}-\lambda'\varepsilon_{l_0})}\left(U_{E_1E_2}\right)_{f_2^2f_1^1,f_1^1f_2}\left(U_{SE_1}\right)_{k_0f_1^1,i_0f_1}\rho_{i_0,j_0}\left(U_{SE_1}\right)^\dagger_{j_0h_1,l_1h_1^1} \\
&\times \left(U_{E_1E_2}\right)^\dagger_{h_1^1h_2,h_1^2h_2^1}\left|k_0,f_1^2,f_2^1,...,f_N,\lambda\right\rangle\left\langle l_0,h_1^2,h_2^1,...,h_N,\lambda'\right| \\
\rightarrow &\sum \rho_{f_1,h_1}\rho_{f_2h_2}\cdots\rho_{f_N,h_N}\rho_{\lambda,\lambda'}e^{i\frac{\chi}{2}(\lambda\varepsilon_{k_0}-\lambda'\varepsilon_{l_0})}\left(U_0^{t_1}\right)_{i_1,k_0}\left(U_{E_1E_2}\right)_{f_2^2f_1^1,f_1^1f_2}\left(U_{SE_1}\right)_{k_0f_1^1,i_0f_1}\rho_{i_0,j_0}\left(U_{SE_1}\right)^\dagger_{j_0h_1,l_1h_1^1} \\
&\times \left(U_{E_1E_2}\right)^\dagger_{h_1^1h_2,h_1^2h_2^1}\left(\left(U_0^{t_1}\right)^\dagger\right)_{l_0,j_1}\left|i_1,f_1^2,f_2^1,...,f_N,\lambda\right\rangle\left\langle j_1,h_1^2,h_2^1,...,h_N,\lambda'\right| \\
\rightarrow &\sum \rho_{f_1,h_1}\rho_{f_2h_2}\cdots\rho_{f_N,h_N}\rho_{\lambda,\lambda'}e^{i\frac{\chi}{2}[\lambda(\varepsilon_{i_1}-\varepsilon_{k_0})-\lambda'(\varepsilon_{j_1}-\varepsilon_{l_0})]}\left(U_0^{t_1}\right)_{i_1,k_0}\left(U_{E_1E_2}\right)_{f_2^2f_1^1,f_1^1f_2}\left(U_{SE_1}\right)_{k_0f_1^1,i_0f_1}\rho_{i_0,j_0} \\
&\times \left(U_{SE_1}\right)^\dagger_{j_0h_1,l_1h_1^1}\left(U_{E_1E_2}\right)^\dagger_{h_1^1h_2,h_1^2h_2^1}\left(\left(U_0^{t_1}\right)^\dagger\right)_{l_0,j_1}\left|i_1,f_1^2,f_2^1,...,f_N,\lambda\right\rangle\left\langle j_1,h_1^2,h_2^1,...,h_N,\lambda'\right|,
\end{aligned}
\tag{A1}
$$

where the summations are over all the indexes in the density matrix element, $(U_{SE_1})_{k_0f_1^1,i_0f_1} = \langle k_0f_1^1|U_{SE_1}|i_0f_1\rangle$, $(U_{E_1E_2})_{f_2^2,f_2^1,f_1^1,f_2} = \langle f_2^2,f_1^1|U_{SE_1}|f_1^1,f_2\rangle$, and $(U_0^{t_1})_{i_1,k_0} = \langle i_1|U_0^{t_1}|k_0\rangle$. In addition, $(U_0^{t_1})_{k_1,i_0}(U_{E_1E_2})_{f_2^2f_1^1,f_1^1f_2}(U_{SE_1})_{i_1f_1^1,k_1f_1} = \gamma^{P_1}_{i_1f_1^2f_2^1,i_0f_1f_2}$ is the probability amplitude of undergoing path P_1: $i_0f_1f_2 \rightarrow k_0f_1^1f_2 \rightarrow k_0f_1^2f_2^1 \rightarrow i_1f_1^2f_2^1$ and $(U_{SE_1})^\dagger_{j_0h_1,l_0h_1^1}(U_{E_1E_2})^\dagger_{h_1^1h_2,f_1^2h_2^1}(U_0^{t_1})_{l_0,j_1} = (\gamma^{P_2}_{j_0h_1h_2,j_1h_2^2h_2^1})^\dagger$ represents the probability amplitude of path P_2: $j_0h_1h_2 \rightarrow l_0h_1^1h_2 \rightarrow l_0h_1^2h_2^1 \rightarrow j_1h_1^2h_2^1$. The generalization of Eq. (A1) to the end of $N-1$ steps is straightforward,

$$
\begin{aligned}
\rho_0 \rightarrow &\sum_{P_1,P_2}\rho_{\lambda,\lambda'}e^{i\frac{\chi}{2}\left[\lambda w_{P_1}^{N-1}-\lambda'w_{P_2}^{N-1}\right]}\Lambda^{P_1}_{i_{N-1}f_{N-1}^3f_N^1,i_0f_1f_2}\rho_{i_0,j_0}\rho_{f_1,h_1}\cdots\rho_{f_N,h_N}\left(\Lambda^{P_2}_{j_0h_1h_2,j_{N-1}h_{N-1}^3h_N^1}\right)^\dagger \\
&\times \left|i_{N-1},f_1^2,f_2^3,\ldots,f_N^1,\lambda\right\rangle\left\langle j_{N-1},h_1^2,h_2^3,\ldots,h_N^1,\lambda'\right|,
\end{aligned}
\tag{A2}
$$

with the probability amplitude $\Lambda^{P_1}_{i_{n-1}f^3_{N-1}f^1_N, i_0 f_1 f_2}$ of transition path P_1: $i_0 f_1 f_2 ... f_N \rightarrow k_0 f^1_1 f_2 ... f_N \rightarrow k_0 f^2_1 f^1_2 ... f_N \rightarrow i_1 f^2_1 f^1_2 ... f_N \rightarrow k_1 f^2_1 f^2_2 ... f_N \rightarrow \cdots \rightarrow i_{N-1} f^2_1, f^3_2 ..., f^3_{N-1} f^1_N$ and the probability amplitude $(\Lambda^{P_2}_{j_0 h_1 h_2, j_{N-1} h^3_{N-1} h^1_N})^\dagger$ of path P_2: $j_0 h_1 h_2 ... h_N \rightarrow l_0 h^1_1 h_2 ... h_N \rightarrow l_0 h^2_1 h^1_2 ... h_N \rightarrow j_1 h^2_1 h^1_2 ... h_N \rightarrow l_1 h^2_1 h^2_2 ... h_N \rightarrow \cdots \rightarrow j_{N-1} h^2_1, h^3_2 ..., h^3_{N-1} h^1_N$. After $N-1$ steps, the work done on the system in paths P_1 and P_2 are $w^{N-1}_{P_1} = \sum^{N-1}_{n=1} \varepsilon_{i_n} - \varepsilon_{k_{n-1}}$ and $w^{N-1}_{P_2} = \sum^{N-1}_{n=1} \varepsilon_{j_n} - \varepsilon_{l_{n-1}}$, respectively,

$$\Lambda^{P_1}_{i_{N-1}f^3_{N-1}f^1_N, i_0 f_1 f_2} = \Pi^{N-1}_{n=2} \gamma^{P_1}_{i_n f^3_n f^1_{n+1}, i_{n-1} f^1_n f_{n+1}} \gamma^{P_1}_{i_1 f^2_1 f^1_2, i_0 f_1 f_2}, \tag{A3}$$

$$\left(\Lambda^{P_2}_{j_0 h_1 h_2, j_{N-1} h^3_{N-1} h^1_N}\right)^\dagger = \left(\gamma^{P_2}_{j_0 h_1 h_2, j_1 h^2_1 h^1_2}\right)^\dagger \Pi^{N-1}_{n=2} \left(\gamma^{P_2}_{j_{n-1} h^1_n h_{n+1}, j_n h^3_n h^1_{n+1}}\right)^\dagger, \tag{A4}$$

where

$$\gamma^{P_1}_{i_1 f^2_1 f^1_2, i_0 f_1 f_2} = \left(U^{t_1}_0\right)_{i_1, k_0} \left(U_{E_1 E_2}\right)_{f^2_1 f^1_2, f^1_1 f_2} \left(U_{SE_1}\right)_{k_0 f^1_1, i_0 f_1} (n=1),$$

$$\gamma^{P_1}_{i_n f^3_n f^1_{n+1}, i_{n-1} f^1_n f_{n+1}} = \left(U^{t_{n+1}}_{t_n}\right)_{i_n, k_{n-1}} \left(U_{E_n E_{n+1}}\right)_{f^3_n f^1_{n+1}, f^2_n f_{n+1}} \left(U_{SE_n}\right)_{k_{n-1} f''_n, i_{n-1} f^1_n} (n>1), \tag{A5}$$

and

$$\left(\gamma^{P_2}_{j_0 h_1 h_2, j_1 h^2_1 h^1_2}\right)^\dagger = \left(U_{SE_1}\right)^\dagger_{j_0 h_1, l_0 h^1_1} \left(U_{E_1 E_2}\right)^\dagger_{h^1_2, h^2_1 h^1_2} \left[\left(U^{t_0}_0\right)^\dagger\right]_{l_0, j_1} (n=1),$$

$$\left(\gamma^{P_2}_{j_{n-1} h^1_n h_{n+1}, j_n h^3_n h^1_{n+1}}\right)^\dagger = \left(U_{SE_n}\right)^\dagger_{j_{n-1} h^1_n, l_{n-1} h^2_n} \left(U_{E_n E_{n+1}}\right)^\dagger_{h^2_n h_{n+1}, h^3_1 h^1_2} \left[\left(U^{t_n}_{t_{n-1}}\right)^\dagger\right]_{l_{n-1}, j_n} (n>1). \tag{A6}$$

After the last steps, Eq. (A2) becomes

$$\rho_0 \rightarrow \sum_{P_1, P_2} \rho_{\lambda, \lambda'} e^{i\frac{\chi}{2}\left[\lambda w^N_{P_1} - \lambda' w^N_{P_2}\right]} \Lambda^{P_1}_{i_N f^2_N, i_0 f_1} \rho_{i_0, j_0} \rho_{f_1, h_1} ... \rho_{f_N, h_N} \left(\Lambda^{P_2}_{j_0 h_1, j_N h^2_N}\right)^\dagger$$

$$\times |i_N, f^3_1, f^3_2, \ldots, f^3_{N-1}, f^2_N, \lambda\rangle\langle j_N, h^2_1, h^3_2, \ldots, h^3_{N-1}, h^2_N, \lambda'|, \tag{A7}$$

where $\Lambda^{P_1}_{i_N f^2_N, i_0 f_1}$ and $(\Lambda^{P_2}_{j_0 h_1, j_N h^2_N})^\dagger$ are defined as

$$\Lambda^{P_1}_{i_N f^2_N, i_0 f_1} = \gamma^{P_1}_{i_N f^2_N, i_{N-1} f^1_N} \Lambda^{P_1}_{i_N f^3_{N-1} f^1_N, i_0 f_1 f_2},$$

$$\left(\Lambda^{P_2}_{j_0 h_1, j_N h^2_N}\right)^\dagger = \left(\Lambda^{P_2}_{j_0 h_1 h_2, j_N h^3_{N-1} h^1_N}\right)^\dagger \left(\gamma^{P_2}_{j_{N-1} h^1_N, j_N h^2_N}\right)^\dagger; \tag{A8}$$

$\Lambda^{P_1}_{i_N f^2_N, i_0 f_1}$ is the probability amplitude of the transition $|i_0, f_1, f_2, \ldots, f_N\rangle \rightarrow |i_N, f^3_1, f^3_2, \ldots, f^2_N\rangle$ and $(\Lambda^{P_2}_{j_0 h_1, j_N h^2_N})^\dagger$ is the probability amplitude from $|j_0, h_1, h_2, \ldots, h_N\rangle$ to $|j_N, h^2_1, h^3_2, ..., h^2_N\rangle$, P_1 in Eq. (A.7) is the path defined by the sequence of states $i_0 f_1 f_2 ... f_N \rightarrow k_0 f^1_1 f_2 ... f_N \rightarrow k_0 f^2_1 f^1_2 ... f_N \rightarrow i_1 f^2_1 f^2_2 ... f_N \rightarrow k_1 f^2_1 f^2_2 ... f_N \rightarrow \cdots \rightarrow i_N f^3_1 f^3_2 ... f^2_N$, and $(\Lambda^{P_2}_{j_0 h_1, j_{N-1} h^1_N})^\dagger$ is the probability amplitude defined by the sequence of states for path P_2: $j_0 h_1 h_2 ... h_N \rightarrow l_0 h^1_1 h_2 ... h_N \rightarrow l_0 h^2_1 h^1_2 ... h_N \rightarrow j_1 h^2_1 h^1_2 ... h_N \rightarrow l_1 h^2_1 h^2_2 ... h_N \rightarrow \cdots \rightarrow j_N h^2_1 h^3_2 ... h^2_N$. Along the paths P_1 and P_2, the work done on the system is $w^N_{P_1} = \sum^N_{n=1} \varepsilon_{i_n} - \varepsilon_{k_{n-1}}$ and $w^N_{P_2} = \sum^N_{n=1} \varepsilon_{j_n} - \varepsilon_{l_{n-1}}$, respectively.

The phase accumulated in the detector can be obtained by tracing out the system degrees of freedom and taking into account Eq. (18),

$$\mathcal{G}_{\chi, \mathcal{W}} = \sum_{P_1, P_2} e^{i\frac{\chi}{2}\lambda\left[w_{P_1} + w_{P_2}\right]} \Lambda^{P_1}_{i_N f^2_N, i_0 f_1} \rho_{i_0, j_0}$$

$$\times \rho_{f_1, h_1} ... \rho_{f_N, h_N} \left(\Lambda^{P_2}_{j_0 h_1, j_N h^2_N}\right)^\dagger, \tag{A9}$$

then the work QPDF is obtained by taking the Fourier transform

$$\mathcal{P}(W) = \sum_{P_1, P_2} \Lambda^{P_1}_{i_N f^2_N, i_0 f_1} \rho_{i_0, j_0} \rho_{f_1, h_1} ... \rho_{f_N, h_N} \left(\Lambda^{P_2}_{j_0 h_1, j_N h^2_N}\right)^\dagger$$

$$\times \delta\left(W - \frac{\lambda}{2}\left[w_{P_1} + w_{P_2}\right]\right). \tag{A10}$$

Since the system degree of freedom is traced out after the last evolution, in paths P_1 and P_2, thus $i_N = j_N$.

[1] J. Birjukov, T. Jahnke, and G. Mahler, Quantum thermodynamic processes: A control theory for machine cycles, Eur. Phys. J. B **64**, 105 (2008).

[2] M. Horodecki and J. Oppenheim, Fundamental limitations for quantum and nanoscale thermodynamics, Nat. Commun. **4**, 2059 (2013).

[3] M. Q. Scully, M. S. Zubairy, G. S. Agarwal, and H. Walther, Extracting work from a single heat bath via vanishing quantum coherence, Science **299**, 862 (2003).

[4] K. Korzekwa, M. Lostaglio, J. Oppenheim, and D. Jennings, The extraction of work from quantum coherence, New J. Phys. **18**, 023045 (2016).

[5] H. Li, J. Zou, W.-L. Yu, B.-M. Xu, J.-G. Li, and B. Shao, Quantum coherence rather than quantum correlations reflect the effects of a reservoir on a system's work capability, Phys. Rev. E **89**, 052132 (2014).

[6] G. Manzano, R. Silva, and J. M. R. Parrondo, Autonomous thermal machine for amplification and

control of energetic coherence, Phys. Rev. E **99**, 042135 (2019).

[7] K. Hammam, H. Leitch, Y. Hassouni, and G. De Chiara, Exploiting coherence for quantum thermodynamic advantage, New J. Phys. **24**, 113053 (2022).

[8] C. L. Latune, I. Sinayskiy, and F. Petruccione, Roles of quantum coherences in thermal machines, Eur. Phys. J. Spec. Top. **230**, 841 (2021).

[9] M. Perarnau-Llobet, K. V. Hovhannisyan, M. Huber, P. Skrzypczyk, N. Brunner, and A. Acín, Extractable work from correlations, Phys. Rev. X **5**, 041011 (2015).

[10] K. Funo, Y. Watanabe, and M. Ueda, Thermodynamic work gain from entanglement, Phys. Rev. A **88**, 052319 (2013).

[11] K. V. Hovhannisyan, M. Perarnau-Llobet, M. Huber, and A. Acín, Entanglement generation is not necessary for optimal work extraction, Phys. Rev. Lett. **111**, 240401 (2013).

[12] L. Bresque, P. A. Camati, S. Rogers, K. Murch, A. N. Jordan, and A. Auffèves, Two-qubit engine fueled by entanglement and local measurements, Phys. Rev. Lett. **126**, 120605 (2021).

[13] P. Solinas, M. Amico, and N. Zanghì, Measurement of work and heat in the classical and quantum regimes, Phys. Rev. A **103**, L060202 (2021).

[14] M. Campisi, P. Hänggi, and P. Talkner, Colloquium: Quantum fluctuation relations: Foundations and applications, Rev. Mod. Phys. **83**, 771 (2011).

[15] P. Talkner, E. Lutz, and P. Hänggi, Fluctuation theorems: Work is not an observable, Phys. Rev. E **75**, 050102(R) (2007).

[16] M. Esposito, U. Harbola, and S. Mukamel, Nonequilibrium fluctuations, fluctuation theorems, and counting statistics in quantum systems, Rev. Mod. Phys. **81**, 1665 (2009).

[17] S. Hernández-Gómez, S. Gherardini, F. Poggiali, F. S. Cataliotti, A. Trombettoni, P. Cappellaro, and N. Fabbri, Experimental test of exchange fluctuation relations in an open quantum system, Phys. Rev. Res. **2**, 023327 (2020).

[18] G. H. Aguilar, T. L. Silva, T. E. Guimarães, R. S. Piera, L. C. Céleri, and G. T. Landi, Two-point measurement of entropy production from the outcomes of a single experiment with correlated photon pairs, Phys. Rev. A **106**, L020201 (2022).

[19] S. Hernández-Gómez, S. Gherardini, N. Staudenmaier, F. Poggiali, M. Campisi, A. Trombettoni, F. S. Cataliotti, P. Cappellaro, and N. Fabbri, Autonomous dissipative Maxwell's demon in a diamond spin qutrit, PRX Quantum **3**, 020329 (2022).

[20] M. Perarnau-Llobet, E. Bäumer, K. V. Hovhannisyan, M. Huber, and A. Acin, No-go theorem for the characterization of work fluctuations in coherent quantum systems, Phys. Rev. Lett. **118**, 070601 (2017).

[21] S. Deffner, J. P. Paz, and W. H. Zurek, Quantum work and the thermodynamic cost of quantum measurements, Phys. Rev. E **94**, 010103(R) (2016).

[22] P. Talkner and P. Hänggi, Aspects of quantum work, Phys. Rev. E **93**, 022131 (2016).

[23] H. J. D. Miller and J. Anders, Time-reversal symmetric work distributions for closed quantum dynamics in the histories framework, New J. Phys. **19**, 062001 (2017).

[24] A. E. Allahverdyan, Nonequilibrium quantum fluctuations of work, Phys. Rev. E **90**, 032137 (2014).

[25] M. Silaev, T. T. Heikkilä, and P. Virtanen, Lindblad-equation approach for the full counting statistics of work and heat in driven quantum systems, Phys. Rev. E **90**, 022103 (2014).

[26] M. Lostaglio, A. Belenchia, A. Levy, S. Hernández-Gómez, N. Fabbri, and S. Gherardini, Kirkwood-Dirac quasiprobability approach to the statistics of incompatible observables, Quantum **7**, 1128 (2023).

[27] S. Hernández-Gómez, S. Gherardini, A. Belenchia, M. Lostaglio, A. Levy, and N. Fabbri, Projective measurements can probe non-classical work extraction and time-correlations, arXiv:2207.12960.

[28] G. Francica and L. Dell'Anna, Quasiprobability distribution of work in the quantum Ising model, Phys. Rev. E **108**, 014106 (2023).

[29] A. M. Gleason, Measures on the closed subspaces of a Hilbert space, J. Math. Mech **6**, 885 (1957).

[30] R. Alicki, The quantum open system as a model of the heat engine, J. Phys. A: Math. Gen. **12**, L103 (1979).

[31] R. Kosloff, A quantum mechanical open system as a model of a heat engine, J. Chem. Phys. **80**, 1625 (1984).

[32] F. W. J. Hekking and J. P. Pekola, Quantum jump approach for work and dissipation in a two-level system, Phys. Rev. Lett. **111**, 093602 (2013).

[33] J. M. Horowitz, Quantum-trajectory approach to the stochastic thermodynamics of a forced harmonic oscillator, Phys. Rev. E **85**, 031110 (2012).

[34] J. J. Alonso, E. Lutz, and A. Romito, Thermodynamics of weakly measured quantum systems, Phys. Rev. Lett. **116**, 080403 (2016).

[35] C. Elouard, D. A. Herrera-Mart, M. Clusel, and A. Auffves, The role of quantum measurement in stochastic thermodynamics, npj Quantum Inf. **3**, 9 (2017).

[36] K. Funo and H. T. Quan, Path integral approach to quantum thermodynamics, Phys. Rev. Lett. **121**, 040602 (2018).

[37] M. Popovic, M. T. Mitchison, A. Strathearn, B. W. Lovett, J. Goold, and P. R. Eastham, Quantum heat statistics with time-evolving matrix product operators, PRX Quantum **2**, 020338 (2021).

[38] A. Levy and M. Lostaglio, Quasiprobability distribution for heat fluctuations in the quantum regime, PRX Quantum **1**, 010309 (2020).

[39] K. Micadei, G. T. Landi, and E. Lutz, Quantum fluctuation theorems beyond two-point measurements, Phys. Rev. Lett. **124**, 090602 (2020).

[40] S. Gherardini, A. Belenchia, M. Paternostro, and A. Trombettoni, End-point measurement approach to assess quantum coherence in energy fluctuations, Phys. Rev. A **104**, L050203 (2021).

[41] A. Sone, Y.-X. Liu, and P. Cappellaro, Quantum Jarzynski equality in open quantum systems from the one-time measurement scheme, Phys. Rev. Lett. **125**, 060602 (2020).

[42] P. Solinas, D. V. Averin, and J. P. Pekola, Work and its fluctuations in a driven quantum system, Phys. Rev. B **87**, 060508(R) (2013).

[43] P. Solinas and S. Gasparinetti, Full distribution of work done on a quantum system for arbitrary initial states, Phys. Rev. E **92**, 042150 (2015).

[44] P. Solinas and S. Gasparinetti, Probing quantum interference effects in the work distribution, Phys. Rev. A **94**, 052103 (2016).

[45] P. Solinas, M. Amico, and N. Zanghì, Quasiprobabilities of work and heat in an open quantum system, Phys. Rev. A **105**, 032606 (2022).

[46] G. Lindblad, On the generators of quantum dynamical semi-groups, Commun. Math. Phys. **48**, 119 (1976).

[47] J. J. Hope, Theory of input and output of atoms from an atomic trap, Phys. Rev. A **55**, R2531 (1997).

[48] B. Bylicka, D. Chruściński, and S. Maniscalco, Non-Markovianity and reservoir memory of quantum channels: A quantum information theory perspective, Sci. Rep. **4**, 5720 (2014).

[49] Z.-X. Man, Y.-J. Xia, and R. Lo Franco, Cavity-based architecture to preserve quantum coherence and entanglement, Sci. Rep. **5**, 13843 (2015).

[50] R. Lo Franco, Nonlocality threshold for entanglement under general dephasing evolutions: A case study, Quantum Inf. Process **15**, 2393 (2016).

[51] L. Aolita, F. de Melo, and L. Davidovich, Open-system dynamics of entanglement: A key issues review, Rep. Prog. Phys. **78**, 042001 (2015).

[52] A. Mortezapour and R. Lo Franco, Protecting quantum resources via frequency modulation of qubits in leaky cavities, Sci. Rep. **8**, 14304 (2018).

[53] B. Bylicka, M. Tukiainen, D. Chruściński, J. Piilo, and S. Maniscalco, Thermodynamic power of non-Markovianity, Sci. Rep. **6**, 27989 (2016).

[54] Z.-X. Man, Y.-J. Xia, and R. Lo Franco, Validity of the Landauer principle and quantum memory effects via collisional models, Phys. Rev. A **99**, 042106 (2019).

[55] S. Lorenzo, R. McCloskey, F. Ciccarello, M. Paternostro, and G. M. Palma, Landauer's Principle in multipartite open quantum system dynamics, Phys. Rev. Lett. **115**, 120403 (2015).

[56] S. Lorenzo, A. Farace, F. Ciccarello, G. M. Palma, and V. Giovannetti, Heat flux and quantum correlations in dissipative cascaded systems, Phys. Rev. A **91**, 022121 (2015).

[57] A. Kutvonen, T. Ala-Nissila, and J. Pekola, Entropy production in a non-Markovian environment, Phys. Rev. E **92**, 012107 (2015).

[58] M. Pezzutto, P. Mauro, and O. Yasser, An out-of-equilibrium non-Markovian quantum heat engine, Quantum Sci. Technol. **4**, 025002 (2019).

[59] P. Marco, P. Mauro, and O. Yasser, Implications of non-Markovian quantum dynamics for the Landauer bound, Quantum Sci. Technol. **18**, 123018 (2016).

[60] R. McCloskey and M. Paternostro, Non-Markovianity and system-environment correlations in a microscopic collision model, Phys. Rev. A **89**, 052120 (2014).

[61] W. H. Louisell, *Radiation and Noise in Quantum Electronics* (McGraw-Hill, San Fransisco, 1964).

[62] V. Vedral, *Modern Foundations of Quantum Optics* (Imperial College Press, London, 2005).

[63] F. Ciccarello, S. Lorenzo, V. Giovannetti, and G. M. Palma, Quantum collision models: Open system dynamics from repeated interactions, Phys. Rep. **954**, 1 (2022).

[64] O. Onishchenko, G. Guarnieri, P. Rosillo-Rodes, D. Pijn, J. Hilder, U. G. Poschinger, M. Perarnau-Llobet, J. Eisert, and F. Schmidt-Kaler, Probing coherent quantum thermodynamics using a trapped ion, arXiv:2207.14325.

[65] J. R. González Alonso, N. Yunger Halpern, and J. Dressel, Out-of-time-ordered-correlator quasiprobabilities robustly witness scrambling, Phys. Rev. Lett. **122**, 040404 (2019).

[66] D. R. M. Arvidsson-Shukur, J. C. Drori, and N. Y. Halpern, Conditions tighter than noncommutation needed for nonclassicality, J. Phys. A: Math. Theor. **54**, 284001 (2021).

[67] H.-P. Breuer, E.-M. Laine, and J. Piilo, Measure for the degree of non-Markovian behavior of quantum processes in open systems, Phys. Rev. Lett. **103**, 210401 (2009).

[68] Z. He, J. Zou, L. Li, and B. Shao, Effective method of calculating the non-Markovianity $\mathcal{N}$ for single-channel open systems, Phys. Rev. A **83**, 012108 (2011).

[69] Z.-X. Man, Y.-J. Xia, and R. Lo Franco, Temperature effects on quantum non-Markovianity via collision models, Phys. Rev. A **97**, 062104 (2018).